Alma Mater Studiorum – Università di Bologna

DOTTORATO DI RICERCA IN

INGEGNERIA ENERGETICA NUCLEARE E DEL CONTROLLO AMBIENTALE

Ciclo XXVI

**Settore Concorsuale di afferenza:** 09/C2

**Settore Scientifico disciplinare:** ING/IND11

# A new method for the estimation of the reverberation time from measured room impulse responses with application to Italian opera houses

Un nuovo metodo per la stima del tempo di riverberazione a partire dalla risposta all'impulso misurata con applicazione ai teatri storici all'italiana

**Presentata da:** **Simona De Cesaris**

**Coordinatore Dottorato**

**Chiar.mo Prof. Antonio Barletta**

**Relatore**

**Chiar.mo Prof. Massimo Garai**

**Esame finale anno 2014**

# A new method for the estimation of the reverberation time from measured room impulse responses with application to Italian opera houses.

# Un nuovo metodo per la stima del tempo di riverberazione a partire dalla risposta all'impulso misurata con applicazione ai teatri storici all'italiana.

Simona De Cesaris

# Contents

# List of Figures

# List of Tables

# Introduction

The Schroeder's backward integration method is the most used method to extract the decay curve of an acoustic impulse response and to calculate the reverberation time from this curve. In the literature the limits and the possible improvements of this method are widely discussed. Nowadays it is the reference method for a wide range of applications and for many standards, e.g. ISO 3382 [1]. Nevertheless, there are critical cases where the Schroeder's method is not easily applicable; also, for some acoustical parameters, like EDT, some doubt may arise about their correct derivation from the Schroeder's integrated curve.

In this work a new method is proposed for the evaluation of the energy decay curve which doesn't make use of an integration over the whole impulse response. On one hand, the aim of this work is to demonstrate that, with some hypotheses, the decay curve extracted with the Schroeder's integration returns the same reverberation time calculated over the energy decay curve extracted with the new method. On the other hand, the present work explains that the envelope calculated with the new method permits to obtain a more detailed energy decay curve; this fact may result in an advantage when dealing with EDT.

In chapter 1 the main literature concerning the energy decay curve extraction is presented. The Schroeder's proposal of a backward integration over the squared impulse response can be considered as the turning point for the extraction of the reverberation time. Due to the importance of the Schroeder's method and to its characteristic to solve at once a series of interrelated problems, since 1965 the literature focused its attention on the limits of this method and on the way to overcome them. In the same chapter, a review of the main improvements of the Schroeder's backward integration method is proposed. Among all of these methods, in the next chapters one will be used that will be referred to as *compensated Schroeder's backward integration method*. At the end of chapter 1, the two criteria extracted from the energy decay curve - reverberation time and EDT - and their comparison are discussed.

In chapter 2 the new proposed method for the energy decay curve extraction is presented. It is called *pre-processed energy detection method, EDM*. The method is discussed in detail: each step of the algorithm is analysed. Also the choice of

the octave band filtering technique is considered, following the classical literature on the subject. The first validation of the new proposed method has been made comparing the results for EDT and reverberation time calculated with the new method and with the best compensated Schroeder's backward integration method, both performed on reference real impulse responses already used in preceding inter-laboratory tests [2] .

Then, both the compensated Schroeder's backward integration method and the *pre-processed energy detection method* have been applied to calculate the reverberation time and the EDT of measured impulse responses. The results of this evaluations and the comparison of the criteria extracted are presented in the second part of this work.

In a third step, a detailed case study has been treated. It consists of a set of nine Italian historical theatres in which acoustical measurements at each seat were carried out by the same team in the past two years (chapter 3). Moreover, the comparison of the two extraction methods has also been applied to a critical case, i.e. the rapidly decaying structural impulse responses of some building elements (chapter 4).

The final parts of the present work deals with the statistical analysis of the reverberation time and EDT values calculated from the impulse responses measurements in the Italian historical theatres (chapter 5). The aim of this evaluation is to know whether a subset of measurements could be considered representative for a complete characterization of this type of opera houses and, if yes, under which conditions. Also in this case the analysis has been done on the values calculated with both the extraction methods.

Given the heterogeneity of the case studies, the characteristics of the new proposed extraction method resulting from the experimental analysis might be considered as its general features.

# Part I

# Theory

# Chapter 1

# Literature

## 1.1 Review of measurement techniques

### 1.1.1 Early methods

The first measurement of reverberation time, as well known, was made in the pioneer work of Sabine. The apparatus used by Sabine [3] consisted of an organ pipe tuned at middle C (512 Hz) controlled by an electro–pneumatic valve and, as microphone, simply the ear. In order to minimize the background noise the measurements were carried out at night. After "several nights practice", the "personal" maximum deviation of the measured reverberation time was estimated by Sabine to be about 0.02 s.

One of the first objective recording setup was described by Meyer in 1927 [4]. It consisted of a microphone, an amplifier and a record oscillograph. The used sound signal was a pure tone and the decay was recorded to a linear scale, obtaining a very irregular decay curve. In order to record a smoother decay curve, Meyer and Just introduced the *warble tone* as sound signal. A warble tone (figure 1.1) is a periodic variation of frequency over a small band which excites a band of frequencies in the room, thus smoothing out the decay.

In 1932 Knudsen [6], taking into account the wave nature of the sound, showed the need of a wide band excitation. In 1931 Hollmann and Schultes [7], switching on–and–off the sound source, produced a *sawtooth* signal [8]. So, in the 1930s, a considerable amount of different "automatic" techniques of measurement was designed [5, 9, 10].

The Hunt's setup (fig. 1.2) consisted of a continuous on-off switching and an automatic averaging over few measurements. In the Hunt's methods the fluctuations are further reduced by: turning off the loudspeaker at the same phase of the sound wave for every decay; rectifying the microphone output and filtering the envelope against the rapid fluctuations about the mean decay; making observa-

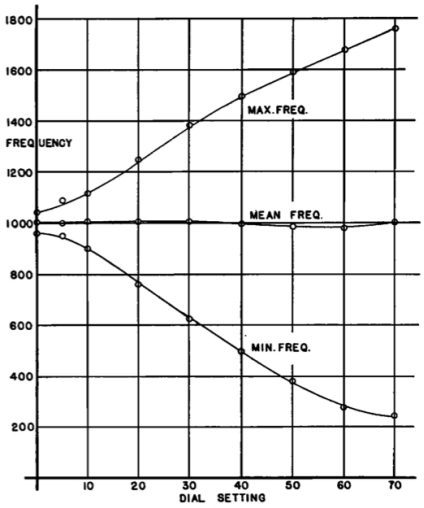


Figure 1.1: Warble tone. After [5].

tions at several microphone positions and averaging a large (40 or more) number of decays for each condition.

The reverberation process is assumed an exponential decay function and the device should provide exponential measurements. Olson and Kreuzer proposed a measurement bridge (fig. 1.3) in which the sound decay is compared with the discharge of a known RC circuit.

A logarithmic level recording device was developed by Ballantine [12]. Meyer and Keidelm [9] developed a logarithmic recording device. They based their instruments on servo principles employing logarithmic input potentiometers, thus allowing to change the dynamic range by changing the input potentiometers.

The chronographic method (also defined *mechanical ear* with reference to the Sabine technique) of Wente and Bedell [10] is shown in fig. 1.4. The signal microphone T, amplified and rectified, passes through the receiving winding of a relay R. When the rectified current exceeds a set value, the relay opens the contact A and the condenser C is charged from the battery E. When the current falls below a set value, the armature the condenser C discharges through the primary winding of the spark coil M and so the stylus P writes on a rotating drum D. In order to have a smoother decay, a LC filter may be inserted between the rectifier and the relay window. In case of noisy rooms the authors suggest the use of a Helmoltz resonator placed over the microphone. The time constant of the resonator is in general shorter than the room one and so a negligible error is introduced.

This apparatus was improved by Bedell and Swartzell increasing the speed of the rotating drum and using a light-weight arm on the stylus [13]. On one hand decay rates up to 600 dB per second could be performed by this high speed level

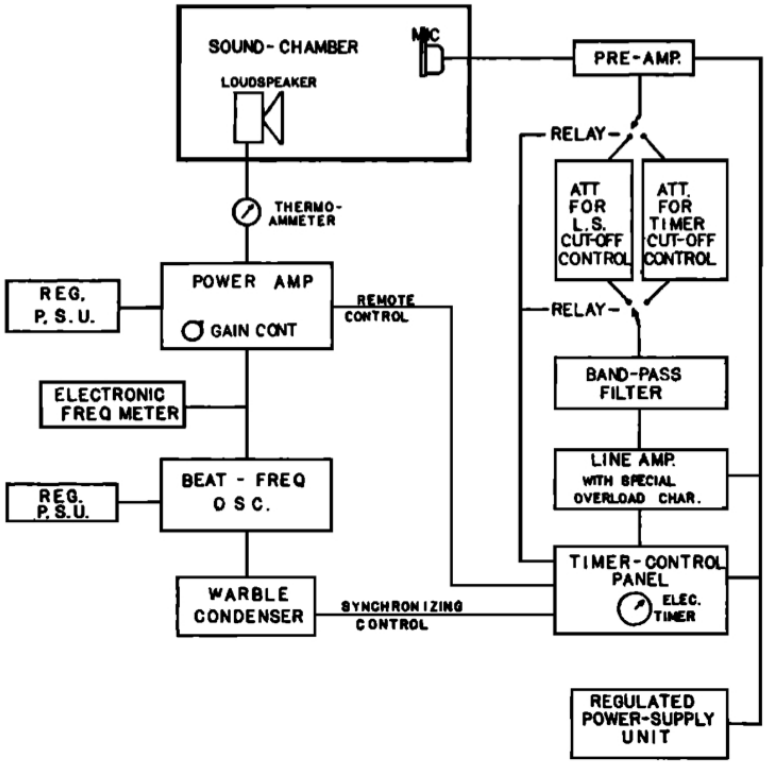


(a) Scheme of the setup.

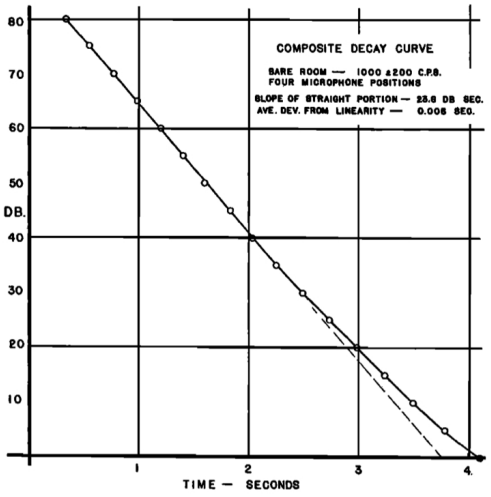


(b) Average of the individual decay curves.

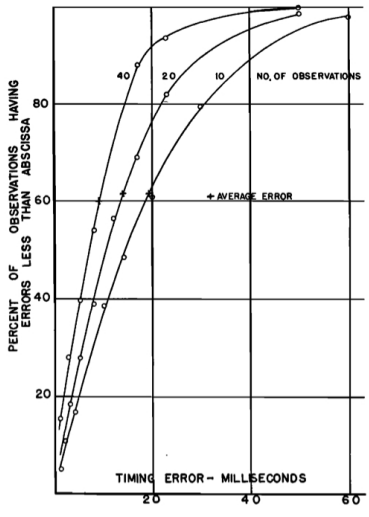


(c) Error distribution curve.

Figure 1.2: Hunt's apparatus for reverberation time measurements [5].

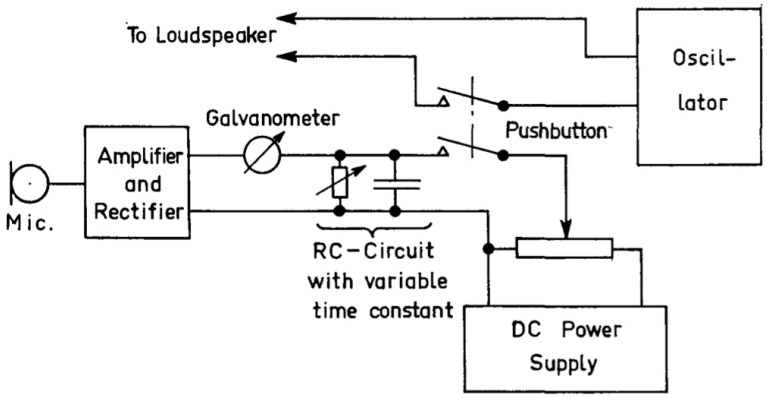


Figure 1.3: Measurement bridge used by Olson and Krezuer [11].

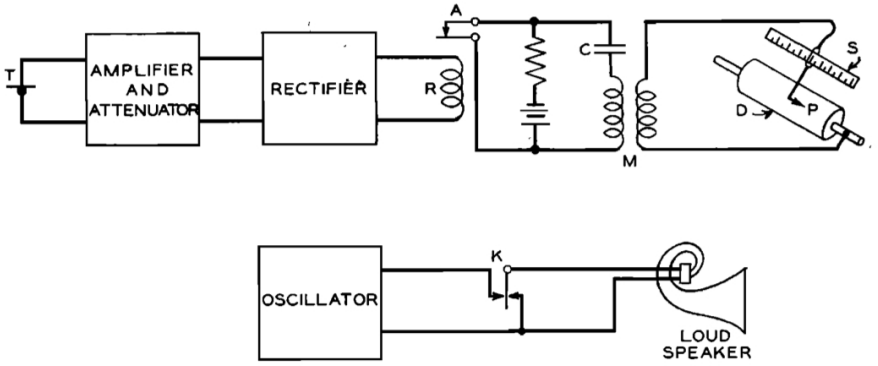


(a) The apparatus.

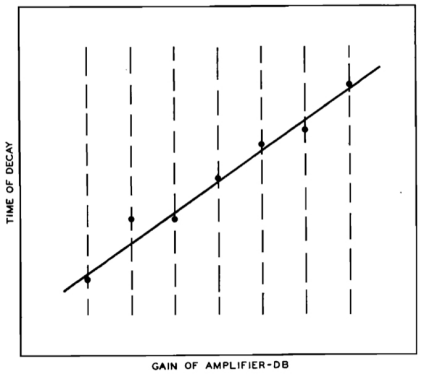


(b) A measured decay.

Figure 1.4: Chronographic method used by Wente and Bedell. After [10].

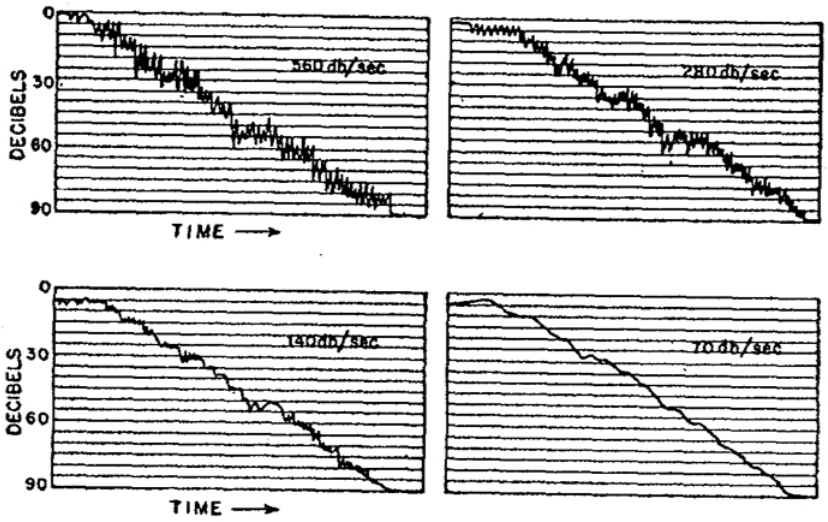


Figure 1.5: High speed level recorder by Bedell and Swartzell [13]. The same sound decay recorded at different speed of the rotating drum have different degree of fluctuations.

recorder. On the other hand, by varying the writing speed of the rotating drum, different degrees of fluctuations of the decay curve may be retained [13, 14].

In the cited work of Knudsen [6], a different way to analyze the sound decay was used: the oscillograms. Writing the amplitude of the pressure vs. the decay time, this method permits the study of the decay modes, as shown in Fig. 1.6. A similar study was made by Wente and others about the "transmission line" [10] of a room. In this last case the Wente's high speed sound level recorder was used and the discontinuity in the so calculated decay curve was used to study the modal characteristics of the room.

In the early 30s the reverberation time was measured almost always in a reverberant chamber in order to extract the absorption coefficient of a specific material. The accuracy of the results allowed the evaluation of the influence quantities, as the temperature or relative humidity, in the $m$ correction factor of the eq. 1.1 [15].

$$T = 0.16 \frac{V}{A + 4mV} \tag{1.1}$$

where $T$ is the reverberation time (s), $V$ is the room volume ($m^3$), $A$ is the equivalent absorption area ($m^2$).

Knudsen [6] was the first to perform measurements of the reverberation time in the concert halls and not only in the reverberant chamber. As already cited, the Knudsen measurements of the sound decay [6] allowed the first analyses of the

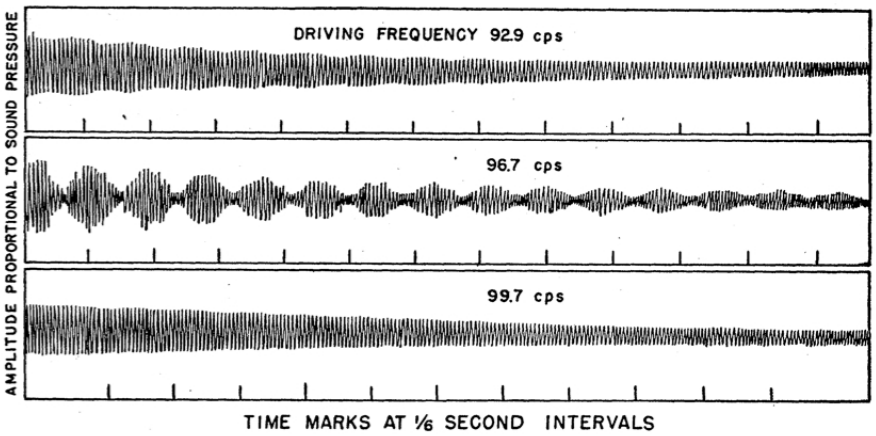


Figure 1.6: Oscillograms used by Knudsen [6]. In the first and in the third sound decay one only mode was excited. In the second sound decay two modes are excited and the oscillogram shows the beats between the two natural frequencies.

decays in the modal region at low frequencies. In the 1936 Lifshitz [16] proposed an early extensive review of the optimum reverberation times, from broadcasting studios to concert halls, proving to be able to measure a wide range of reverberation times in wide frequency ranges.

### 1.1.2 The Schroeder's integration and the analog measurement techniques

After World War II the measurement techniques have been improved by the use of magnetic tapes. Developed in Germany in the 30s, the magnetic tape permits the recording of the sound decay. From the same recording of the decay, different analyses may be performed at a later time, e.g. the analysis of wide or narrow band filtered decays. The use of the white noise (or shot) instead of pure (or warble) tone [8] was allowed by the new large band loudspeakers.

The set-up of a reverberation chamber in the early '60s (meaning by that sources and receivers) is quite similar to one of those in use today (fig. 1.8a. In this technical era the Schroeder's backward integration (see section 1.2) was published. A technical implementation of the backward integration is shown in the fig. 1.8b: the negative sign is due to the inverse sense of the tape scrolling, the squaring block is realized by a diode bridge and the integration was made with a RC filter with a high time constant.

The transistors replaced the vacuum tube in the equipments: preamplifiers [17] and non-linear components [18] allowed lower noise floor level in the decay measurements. In these years the focus on the noise floor rose because the decay

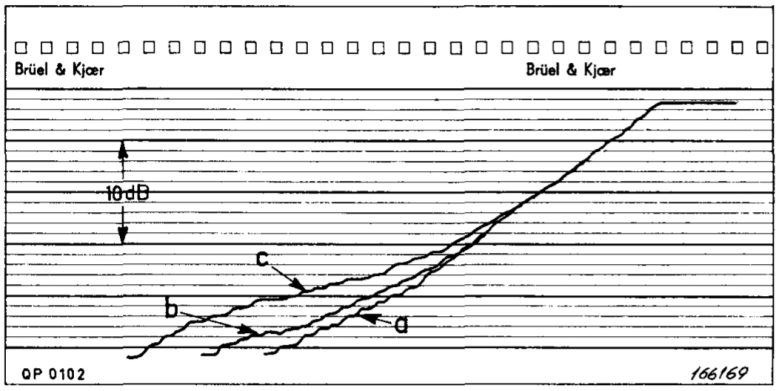


Figure 1.7: Decay curves extracted with the backward integration method starting at different time instants. After [19].

curve extracted with backward integration responded to the noise floor level (fig. 1.8c).

Schroeder's proposal opened a new era in the reverberation time evaluation. The scientific community soon recognized the importance of the new method and the discussion on possible improvements started to take place. In 1966, only one year after the Schroeder's publication [20], the error introduced by the noise floor in the decay evaluation was underlined and the first attempt to solve this problem was to use different starting times of backward integration (fig. 1.7).

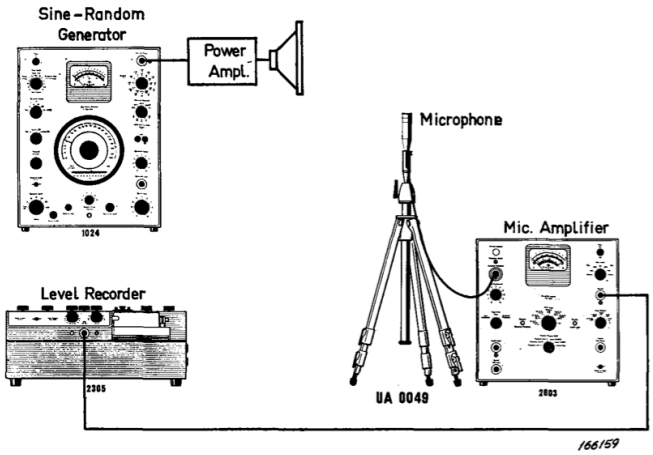


(a) Sound decay recording.

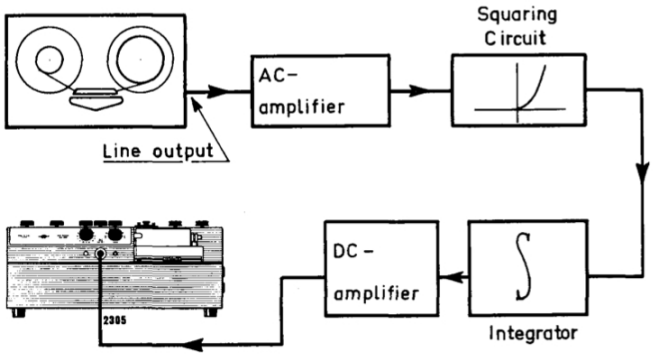


(b) Backward integration.

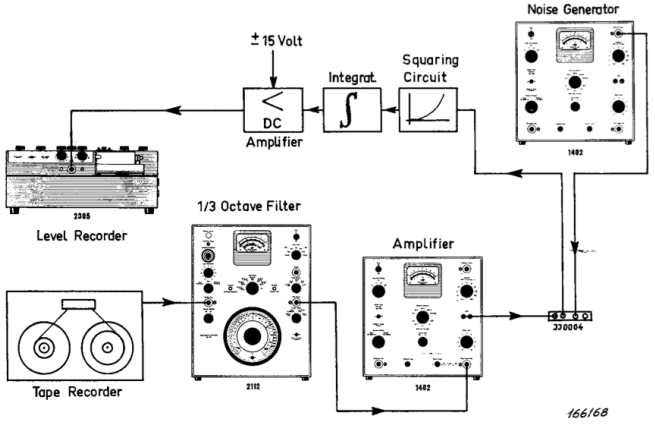


(c) Measurement of the noise floor level.

Figure 1.8: Analog measurement equipments in a Brüel & Kjær technical review of 1966 [19].

## 1.2 Schroeder's backward integration

In 1965 Schroeder proposed a new method of measuring reverberation time [20].

With the classical method, the accuracy with which the reverberation time could be determined from the decay curve was limited by random fluctuations in the decay curves. In 1965 the most frequently used method to minimize the effect of these fluctuations was to repeat the measurements many times and to average the reverberation times or the decay rates obtained from the individual decay curves. To extract more and more useful information from the decay curve, the best way was to average many curves obtained under identical physical conditions and not just the decay rates or the reverberation times obtained from individual decay curves. Unfortunately, averaging over many decay curves was rather impractical.

The new method of measuring reverberation time, proposed by Schroeder in 1965, yields in a single measurement a decay curve that in principle is identical to the average over infinitely many decay curves that would be obtained exciting the enclosure with bandpass filtered noise.

Schroeder demonstrates that

$$\left\langle s^2(t) \right\rangle = \int_t^\infty r^2(x)dx \tag{1.2}$$

where

$\langle s^2(t) \rangle$ is the ensemble average of the squared noise decay;

$r^2(t)$ is the squared impulse response.

This is a considerable improvement over the previous methods because it permits to evaluate the decay curve measuring only an impulse response and then post processing the measured data.

## 1.3 Improvements of Schroeder's method

Since the next year of the Schroeder's method proposal, many authors studied and discussed the critical features of the method and proposed different improvements, e.g. [21, 22, 23, 24].

As shown in figure 1.9, the reverberation time estimated with the classical implementation of the Schroeder's backward integration method could have some problems. The main problem is related to the noise always present in a measured impulse response [25]: the noise level reduces the useful dynamic range. In extreme cases the decay range becomes so small that it is not possible to evaluate any reverberation time. In fact, mathematically the upper limit of integration is infinity that corresponds to the end of the impulse response under test. It is evident that if the time length of the impulse response is greater than the energy decay time, the

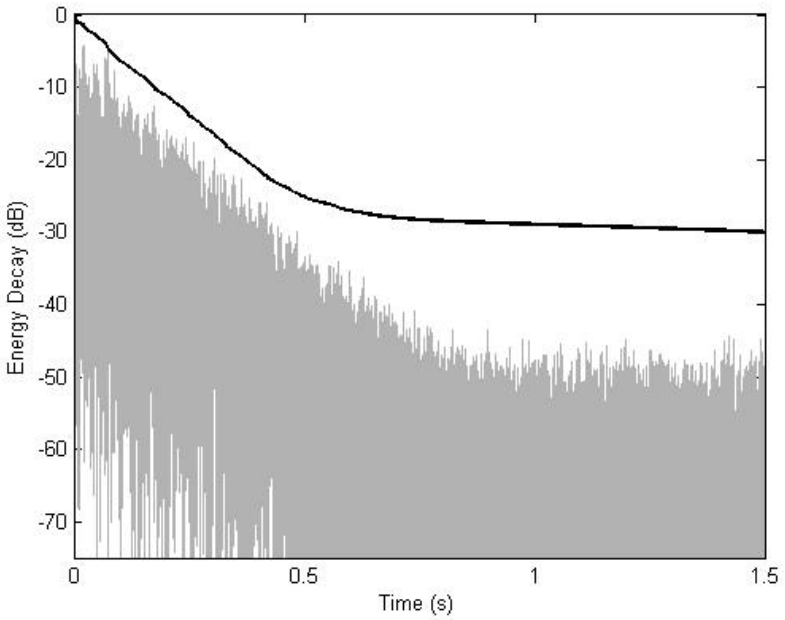


Figure 1.9: Test impulse response. Grey curve: normalized impulse response. Black curve: classical Schroeder's backward integral.

last part of the impulse response contains only noise. Integrating all this noise, the resulting backward integral overestimates the real energy decay time; the evaluable dynamic range is reduced.

Another problem can be identified in the fact that the decay approaches minus infinity at the upper limit of integration ($t_{ULI}$) and returns the reverberation time value even if the signal to noise ratio is insufficient.

Several authors in literature underlined the above-mentioned problems of the classical Schroeder's backward integration implementation and proposed different methods to overcome these limits and calculate a correct decay time with the maximum decay range available.

Guski and Vorländer in 2014 [26] makes a complete review of the most used literature methods proposed to overcome the classical Schroeder's integration limits: here a summary of each of these methods is presented in the following.

**Truncation at intersection time** The first idea to overcome the limits of the Schroeder's classical implementation and in particular the problem related to the integration of the background noise, is to truncate the impulse response at the intersection time $t_i$ that becomes the new upper limit of integration. The

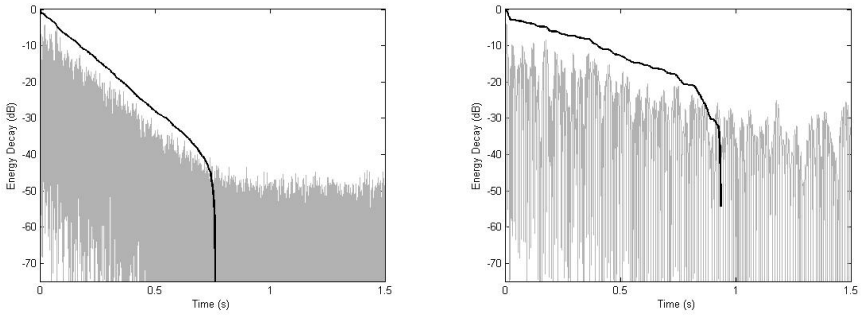


(a) Proper evaluation. (b) Critical evaluation.

Figure 1.10: Test impulse response. Grey curve: normalized impulse response. Black curve: Compensated Schroeder's backward integral with trucation at intersection time.

Schroeder's integration becomes:

$$E(t) = \int_t^{t_i} p^2(\tau) d\tau \tag{1.3}$$

Thus, this method defines the integration limit at $t_i$ that is defined as the intersection time between the decay and the noise floor.

Different proposals have been made for the identification of this intersection time. For example, Faiget [27] calculated the value of $t_i$ as the intersection point between the two straight lines representing respectively the regression line made on the decay and the line $5\,dB$ above the background noise. The regression line is defined as the range between the direct sound and six times the time corresponding to the mean free path.

The noise error in the energy decay curve is reduced drastically (fig. 1.10a), but the truncation introduces a further error. The energy decay curve is approaching minus infinity because of the missing signal energy from the truncation time to infinity. The unlimited dynamic range of the resulting energy decay curve always allows an evaluation of the energy decay curve, even if the signal to noise ratio is insufficient for a certain reverberation time. An example is shown in figure 1.10b: the intercept between the curve and the level of -35 dB exists, but it is not representative of the real energy decay. Thus the evaluation of the reverberation time as $T_{30}$ returns a value, but it is wrong (it is expected that the method doesn't return any value if the dynamic range is insufficient).

**Truncation and correction** In order to improve the truncation procedure, Lundeby et al. [28] proposed a correction term to prevent the truncation error.

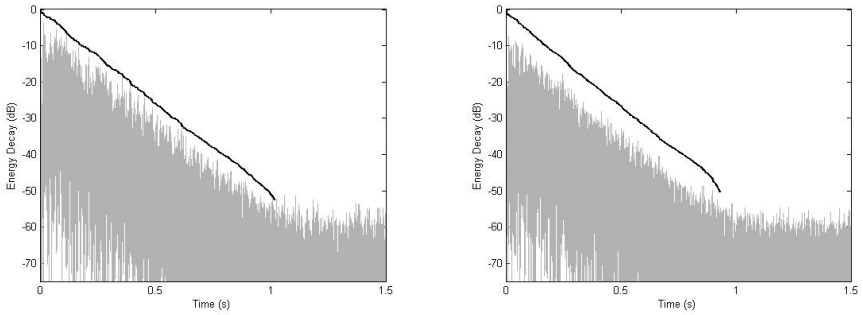


(a) Proper evaluation. (b) Critical evaluation.

Figure 1.11: Test impulse response. Grey curve: normalized impulse response. Black curve: Compensated Schroeder's backward integral with trucation at intersection time and correction.

The missing signal energy from truncation time to infinity $C_{comp}$ is estimated and added to the truncated integral. The estimation of the energy decay curve becomes:

$$E(t) = \int_t^{t_i} p^2(\tau) d\tau + C_{comp} \tag{1.4}$$

Moreover, Lundeby et al. suggested to leave a safety margin of 5 - 10 dB above the level corresponding to the intersection time to reduce the influence of the noise. In fact, defining the intersection time as the one where the signal equals the noise, the signal part is already influenced by noise. For this reason, here $t_i$ is defined as the time corresponding to a level of 10 dB above the intersection time between signal and noise level.

$C_{comp}$ is estimated assuming exponential decay. At the zero point the energy density is known (it is the coefficient of the regression line $B$) and at the intersection point $t_i$ the energy density is assumed as the mean noise energy density $N$ [28]. Assuming the exponential decay $r(t) = Be^{At}$ where $B$ is known and $A = \frac{ln(N/B)}{t_i}$, then

$$C_{comp} = -\frac{B}{A} e^{At_i} \tag{1.5}$$

The compensation $C_{comp}$ eliminates the truncation error as shown in figure 1.11a. In this case the dynamic range of the energy decay curve is limited according to the signal to noise ratio and the problem related to the evaluation of the reverberation time when the dynamic range is insufficient is eliminated. A slight overestimation is possible due the background noise estimation before the truncation: one example is presented in figure 1.11b.

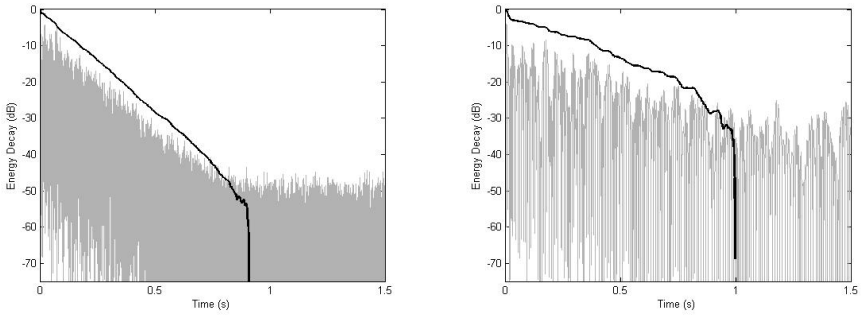


(a) Proper evaluation. (b) Critical evaluation.

Figure 1.12: Test impulse response. Grey curve: normalized impulse response. Black curve: Compensated Schroeder's backward integral with subtraction of noise.

**Subtraction of noise** Instead of truncating the impulse response evaluating the intersection time between the noise floor level and the signal, Chu in 1978 [29] proposed the "subtraction of noise method" where the noise floor level is subtracted.

The decay curve of a noisy impulse response can be written as:

$$E(t) = \int_t^{t_{IR}} (p_d(\tau) + n(\tau))^2 d\tau = \int_t^{t_{IR}} (p_d^2(\tau) + 2p_d(\tau)n(\tau) + n^2(\tau))d\tau \qquad (1.6)$$

where $p_d(\tau)$ is the impulse response without noise and $n(\tau)$ is the additive noise in the impulse response. As $n(\tau)$ can be either positive or negative, the second term integrated will return zero. The third term always gives a positive contribution in particular for large $\tau$. The noise level $N_{est}$ can be estimated for large $\tau$ after the response $p_d(\tau)$ has vanished. It can be calculated as a temporal average of the last part of the impulse response, where only background noise is present. $N_{est}$ is then subtracted from the impulse response before the backward integration:

$$E(t) = \int_t^{t_{IR}} (p^2(\tau) - N_{est}^2)d\tau \qquad (1.7)$$

where $p(\tau)$ is the noisy impulse response.

Comparing figures 1.9 and 1.12a, the advantages of using the noise compensation method instead of the uncompensated Schroeder's backward integration method are evident.

By subtracting the estimated noise level, the distribution of the new noise component can be considered as zero mean. The noise error is reduced by temporal averaging during the integration (fig. 1.12a).

This technique works well for the first part of the impulse response where the signal energy is dominant. For the later part this method fails because, as for the truncation method, the energy decay curve approaches minus infinity. Likewise the truncation method, the problem of an unlimited dynamic range of energy decay curve occurs: for example in figure 1.12b the estimation of reverberation time $T_{30}$ is incorrect due to the intersection at $-35\,dB$ in the region where the decay curve is no more representative of the real impulse response.

**Truncation, correction and subtraction** The method is a combination of all the techniques mentioned above: the estimated noise level is subtracted, the impulse response is truncated at the intersection time and the correction for the truncation is applied. The resulting energy decay curve is:

$$E(t) = \int_t^{t_i} (p^2(\tau) - N_{est}^2) d\tau + C_{comp} \tag{1.8}$$

This implementation permits to take advantage of all the previous presented methods: the influence of noise is minimized by subtracting the noise level. The truncation of the impulse response suppresses errors in the later part of the room impulse response. The subtraction of noise minimizes the problem related to the evaluation of the noise floor level and the compensation avoids that the energy decay curve approaches minus infinity (fig. 1.13).

Among all the improvements of the Schroeder's backward integration method, this is the one that returns the best evaluation of the energy decay curve with a dynamic range directly corresponding to the signal to noise ratio.

### 1.3.1 Envelope based methods

The correction method presented by Lundeby et al. [28] is the first step of a complete method for the extraction of the energy decay curve: the different steps of this methods suggest that it could be seen as an envelope based method. In particular it is a method that, correcting the background noise, consists in an iterative algorithm to obtain an envelope curve. After the averaging of the squared impulse responses locally using a static defined width of the window of 10-50 ms, it estimates the background noise level as the one of the last 10% of the impulse response. Then the slope of the decay is estimated from 0 dB to 5 or 10 dB above the noise level. Through this slope, a new time interval length is defined for the averaging of the squared impulse response. These steps have to be iterated and

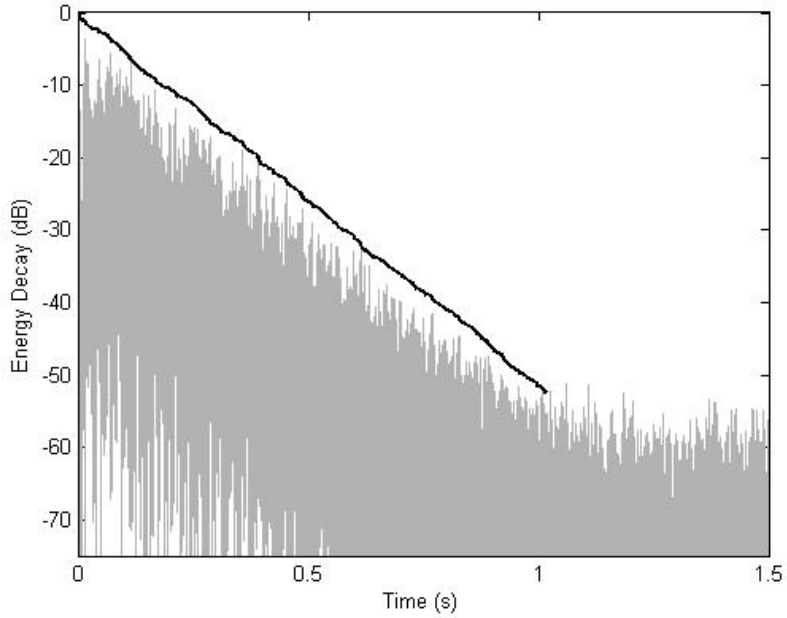


Figure 1.13: Test impulse response. Grey curve: normalized impulse response. Black curve: Compensated Schroeder's backward integral with subtraction of noise, truncation at intersection time and correction.

Lundeby et al. suggests that 5 iterations could be enough for the convergence of the energy decay curve to the energy decay of the impulse response.

Satoh [30] proposed another method to obtain the reverberation time directly from the squared impulse response. The focus of the method is to obtain an envelope of the impulse response by calculating the root mean square value for every 10 ms.

## 1.4 Non linear methods - The Bayesian estimation

Under noisy conditions, the successful application of the Schroeder's method with the different correction methods requires a careful choice of the integration limit or a precise estimate of the mean-square value of the background noise. To overcome these problems, in 1995 Xiang [31] proposed an alternative method using a non-linear iterative regression approach for evaluating reverberation time from Schroeder's decay curve.

The decay function model established in [31] has been extended to multirate decay functions [32, 33, 34]: Xiang demostrated that a model-based analysis using Bayesian probability theory is well suited to determine decay times from measurements in coupled spaces.

A multirate decay function can be modeled as

$$F(\mathbf{A}, \mathbf{T}, t_k) = \sum_{j=1}^{m} A_j G_j(T_j, t_k) \tag{1.9}$$

where

$$G_j(T_j, t_k) = \begin{cases} e^{\frac{-13.8 t_k}{T_j}}, & \text{for j=1,2,..,m-1} \\ L - t_k, & \text{for j=m} \end{cases} \tag{1.10}$$

and $\mathbf{A} = \{A_1, A_2, .., A_m\}$, $\mathbf{T} = \{T_1, T_2, .., T_m\}$ and $T_i$ is the $i$th decay time to be estimated. The $A_j$ are the linear parameters and $T_j$ are non-linear parameters. In equation 1.10 $L$ represents the upper limit of integration of the Schroeder's decay curve.

The decay model approximates Schroeder's decay function

$$d_k = F(\mathbf{A}, \mathbf{T}, t_k) + \epsilon_k \tag{1.11}$$

in such a way that $F(\mathbf{A}, \mathbf{T}, t_k)$ models Schroeder's decay function with error $\epsilon_k$.

Given Schroeder's decay function data $\mathbf{D} = \{d_1, d_2, .., d_K\}$ obtained from experimental measurements, and the background information $I$, the joint probability

of all the model parameters $p(\mathbf{A}, \mathbf{T} \mid \mathbf{D}, I)$ expresses the probability that the given model in equation 1.10 accurately describes the physical situation. Accordingly to Bayes theorem it can be written as

$$p(\mathbf{A}, \mathbf{T} \mid \mathbf{D}, I) = \frac{p(\mathbf{A}, \mathbf{T} \mid I) p(\mathbf{D} \mid \mathbf{A}, \mathbf{T}, I)}{p(\mathbf{D} \mid I)} \tag{1.12}$$

where $p(\mathbf{A}, \mathbf{T} \mid I)$ is the joint probability density of $\mathbf{A}$ and $\mathbf{T}$ given the background information $I$, that is the *prior* probability, the probability $p(\mathbf{D} \mid \mathbf{A}, \mathbf{T}, I)$ is the *likelihood* distribution for the data if the values parameter of the model are known. The probability $p(\mathbf{A}, \mathbf{T} \mid \mathbf{D}, I)$ is called the posterior probability.

The probability $p(\mathbf{D} \mid I)$ is called *evidence* and could be considered as a constant that normalizes the product of the prior and the likelihood.

On the application level, the matrix formulation is more useful [35]. For this formulation, equation 1.10 becomes

$$G_k j(T_j, t_k) = \begin{cases} t_K - t_k, & \text{for j=0} \\ e^{\frac{-13.8 t_k}{T_j}}, & \text{for j=1,2,..,m-1} \end{cases} \tag{1.13}$$

where $G_k j(T_j, t_k)$ is the $j$th column of $\mathbf{G}$ that is a matrix $K \times m$.

The model function in 1.9 becomes $\mathbf{GA}$ where $\mathbf{A}$ is a column vector of $m$ coefficients, termed *linear parameter vector* and equation 1.11 becomes

$$\mathbf{D} = \mathbf{GA} + \mathbf{e} \tag{1.14}$$

where $\mathbf{D}$ is a column vector of $K$ elements with the Schroeder's decay function data and $\mathbf{e}$ is the error vector that could be rewritten as

$$\mathbf{e} = \mathbf{D} - \mathbf{Q}\alpha \tag{1.15}$$

where

$$\mathbf{Q} = \mathbf{GE}\boldsymbol{\Delta}^{-1} \tag{1.16}$$

and

$$\alpha = \boldsymbol{\Delta}\mathbf{EA} \tag{1.17}$$

where $\mathbf{E}$ is a square matrix containing $m$ eigenvectors and $\boldsymbol{\Delta}^{Tr}\boldsymbol{\Delta} = \boldsymbol{\Lambda}$ and $\boldsymbol{\Lambda}$ is a diagonal matrix containing $m$ eigenvalues of the eigenvectors.

With these new formulations, equation 1.12, where $\mathbf{T}$ is a vector of $m$ coefficients called *non-linear parameter vector*, is valid.

Background information $I$ include that the Schroeder's decay model in Eq. 1.13 through Eq. 1.14 describes the data $\mathbf{D}$ reasonably well, thus all errors in $\mathbf{e}$

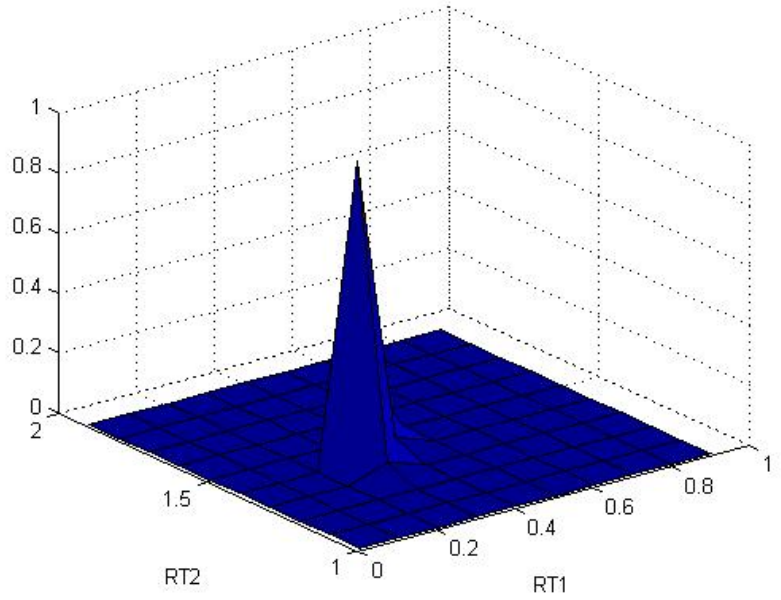


Figure 1.14: 2D posterior probability density function (PPDF) calculated for the test impulse response considering decay rate.

are bounded by a finite value. Given finite error and a reasonable model as the only available information, the application of the principle of maximum entropy [32] assigns a Gaussian distribution to the likelihood function $p(\mathbf{D} \mid, \mathbf{A}, \mathbf{T}, I)$ and the independence of the errors $e_i$ from each other, so that

$$p(\mathbf{D} \mid, \mathbf{A}, \mathbf{T}, \sigma, I) = (\sqrt{2\pi}\sigma)^{-K} exp(\frac{\mathbf{e}^{Tr}\mathbf{e}}{2\sigma^2}) \tag{1.18}$$

with a finite but unspecified error variance $\sigma^2$.
The posterior probability density function (PPDF) becomes

$$p(\alpha, \mathbf{T} \mid \mathbf{D}, \sigma, I) \propto p(\alpha, \mathbf{T} \mid I)(\sqrt{2\pi}\sigma)^{-K} exp(-\frac{(\mathbf{D} - \mathbf{Q}\alpha)^{Tr}(\mathbf{D} - \mathbf{Q}\alpha)}{2\sigma^2}) \tag{1.19}$$

The marginalization over $\alpha$ with a uniform prior and over $\sigma$ by assigning Jeffrey's prior leads to an analytically tractable PPDF in the form of a student-t distribution over only the decay time space

$$p(\mathbf{T} \mid \mathbf{D}, I) \propto \left]\mathbf{D}^{Tr}\mathbf{D} - \mathbf{q}^{Tr}\mathbf{q}\right[^{\frac{m-K}{2}} \tag{1.20}$$

with

$$\mathbf{q} = \mathbf{Q}^{Tr}\mathbf{D} \tag{1.21}$$

The student-t distribution in Eq. 1.20 over an $n$-dimensional decay time space demonstrates $n!$ distinctly separated modes of equal height. Only one mode serves to the estimation purpose, so the localization of the peak position of one of these modes will provide the estimation of decay times. In figure 1.14 is shown an example of PPDF with two dimensions that permits to evaluate two different reverberation times (RT1 and RT2 in the figure) corresponding to the coordinates of the peak.

**Discussion** The bayesian method proposed by Xiang returns a good evaluation of different values of reverberation time for each impulse response under test. Xiang extended the method with an algorithm able to estimate also the number of decay rates useful for a complete characterization of a particular impulse response.

On the other hand the method is computationally heavy and requires specific techniques for the evaluation with more than two or three dimensions of the PPDF (conseguently two or three decay rates to estimate).

Another feature of the Xiang method is that it does not only return the decay rates but also the corresponding decay ranges. This could be seen as a good characteristics of the method, but it is difficult to compare the results of the Xiang method with the others, because it does not return the classical reverberation times (for example $T_{15}$ or $T_{30}$), but the decay ranges depend only on the impulse response under test and it is not possible to define them priorly.

## 1.5 ISO 3382 criteria based on EDC

### 1.5.1 Reverberation time

The standard ISO 3382 [1] defines the reverberation time as the duration required for the space-averaged sound energy density in an enclosure to decrease by 60 dB after the source emission has stopped. This definition suggests the evaluation of the reverberation time with the *interrupted noise method*. As previously explained in section 1.2, this method requires lots of measurements for each evaluation. In the same section, a second method to extract the reverberation time was explained: the *integrated impulse response method* proposed by Schroeder in 1965 [20]. Both these methods return the energy decay curve.

For the reasons explained before, in this work only the integrated impulse response method is analysed.

ISO 3382 suggests that within the evaluation range (for example from -5 to -35 dB for the $T_{30}$ evaluation), a least-squares fit line shall be computed for the

curve and then the slope of the straight line gives the decay rate from which the reverberation time is calculated extrapolating the value over 60 dB.

As explained in the previous sections, many studies in literature proposed different methods to overcome the problems related to the classical implementation of Schroeder's backward integration, in order to return a representative value of the reverberation time through a linear fitting over the decay curve.

Xiang in 1995 [31] proposed an alternative method using a non-linear iterative regression approach for evaluating reverberation times from Schroeder's decay curves. Karjalainen [36] then proposed an improved non-linear approach based on the Xiang method. One other observation is that the linear fitting over the Schroeder's decay curve assumes a linear decay: only in those cases when the decay is linear, the linear fitting returns the representative value for the reverberation time. In all the other cases, the liner fitting over the Schroeder's decay curve may not be suitable for the evaluation. Xiang in 2001 [32] and in the subsequent years presented a new method based on the one proposed in 1995 [31] and extended it to multirate decay functions. In 1995 Xiang demonstrated the validity of this method for a coupled space, observing the ability of the method to return the two typical decay rates of a coupled volume. In the subsequent years, Xiang extended the same method for an arbitrary number of decay rates. The method and its extensions are based on the Bayesian probabilistic inference.

### 1.5.2 EDT

In the 60's, it was realised that the reverberation time measured according to the standard method between -5 and -35 dB relative to the initial level might not relate directly to the perceived sense of reverberation. Atal, Schroeder and Sessler [37, 38] conducted subjective tests in which subjects were asked to match artificially reverberated speech and music, with the comparison being made between decays which were linear and non-linear. For these artificially reverberated sounds the decay rate over the first 160 ms was found to relate most closely to perceived reverberation. When recordings were made in two concert halls, the subjective reverberation time matched most closely the initial reverberation time measured over the first 15 dB of the decay. Jordan [39] subsequently proposed in 1969 measuring the decay rate over the first 10 dB of the decay, naming it the *early decay time* (EDT).

In the ISO 3382 the early decay time is defined as the *perceived reverberation* and is evaluated over the decay curve through a linear fitting over the first 10 dB and then extrapolated over 60 dB.

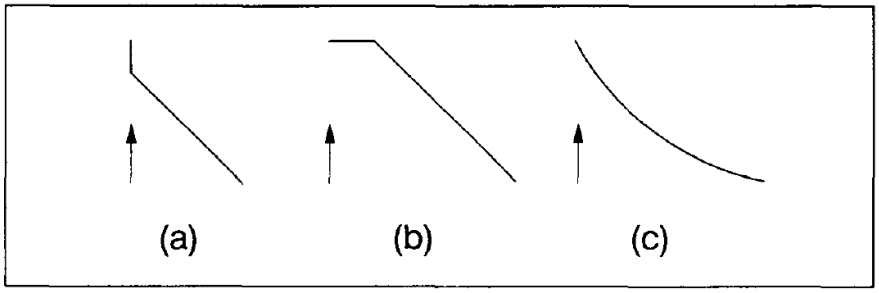


Figure 1.15: Types of early decay curve. The arrow indicates the arrival time of direct sound [40].

## 1.6 Comparison of reverberation time and EDT

It is well known that the early decay time (EDT) is well related to the perceived reverberance [37, 38, 39]. This means that EDT has a particular importance in the evaluation of the acoustic characteristics of an enclosure.

Barron [40] divided the possible effects of early reflections on the decay curve (see fig. 1.15). The three type of early decay are named (a) *Cliff-type decay* (b) *Plateau-type decay* and (c) *Sagging decay*. He explained how the possible distribution of early reflections could be related to each type of early decay:

(a) The *Cliff-type decay* corresponds to very strong early reflections and in this case typically a comparison between EDT and reverberation time reveals that the first is significantly shorter than the second;

(b) The *Plateau-type decay* occurs when first reflections are absent and in this case the EDT is longer than reverberation time;

(c) The *Sagging reverberation curve* is another case where the EDT value is shorter than the reverberation time.

In the same work Barron [40] also made some different evaluations focused on EDT extracted from the measurements performed in 17 different halls. At first he compared the EDT and the reverberation time calculating the ratio $\frac{EDT}{RT}$ and averaging the value in the octave bands from 500 Hz to 2000 Hz. He found that it is possible to divide the halls in three different groups: for most of them the $\frac{EDT}{RT}$ is less than 1, for some other halls the ratio is approximately 1 and only one hall presents a ratio greater that 1 (fig. 1.16).

It is evident that in those halls where the $\frac{EDT}{RT}$ ratio is approximately 1, the field is diffused and there are no strong early reflections.

Of particular interest for the present work is the analysis of those halls where the ratio is less that 1. In this case typically there is a strong early sound and a weak

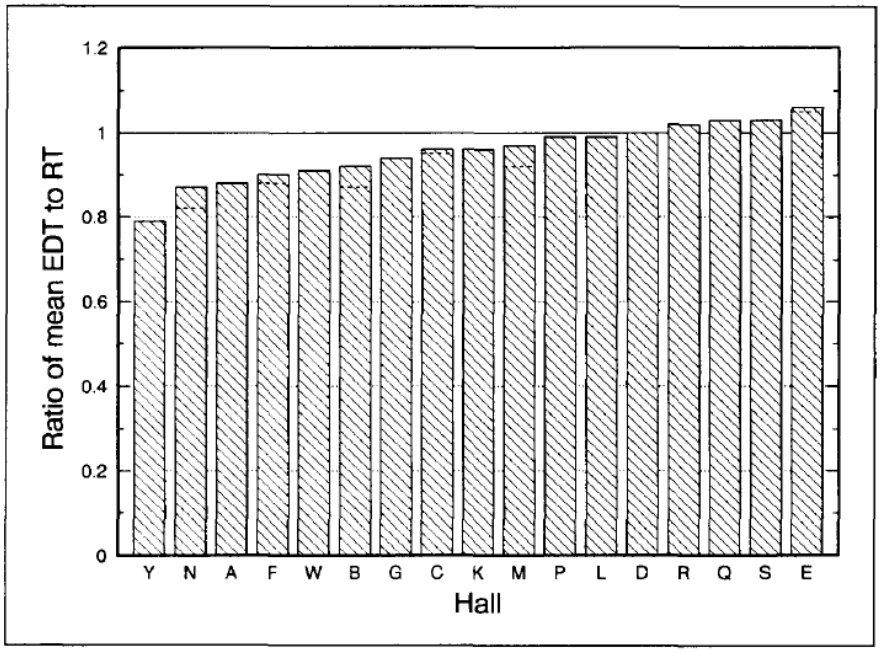


Figure 1.16: Mean EDT-RT ratios in British concert halls at mid frequencies [40].

late sound. Barron relates this effect to the particular geometrical features of the halls. All of these features are focused on the enhancement of the first reflections and on their re-direction to the listening positions through the inclination of the surfaces [41].

Another analysis that Barron performed in the same paper and that is of particular interest for the present work, is the evaluation of early decay time versus source-receiver position (fig. 1.17). For the halls analysed in that work, he found that the EDT values depend on the source-receiver position expecially for those halls with a wide spread of EDT values. Typically, the EDT values decrease increasing the distance between the source and the receiver and the trend is a linear dependence between the two.

On one hand the importance of early decay time is related to its psychological value (it is named *perceived reverberation*). On the other hand, it is related to the objective evaluation of a room: for example the differences between EDT and reverberation time and their ratio assume a specific significance in the characterization of the hall.

This means that it is important to have a good evaluation of early decay time strictly related to the real decay of the impulse response.

Bradley in 2011 [42] said that, although the procedure for determining the EDT seems to be good, some problems could occur expecially for the measurements

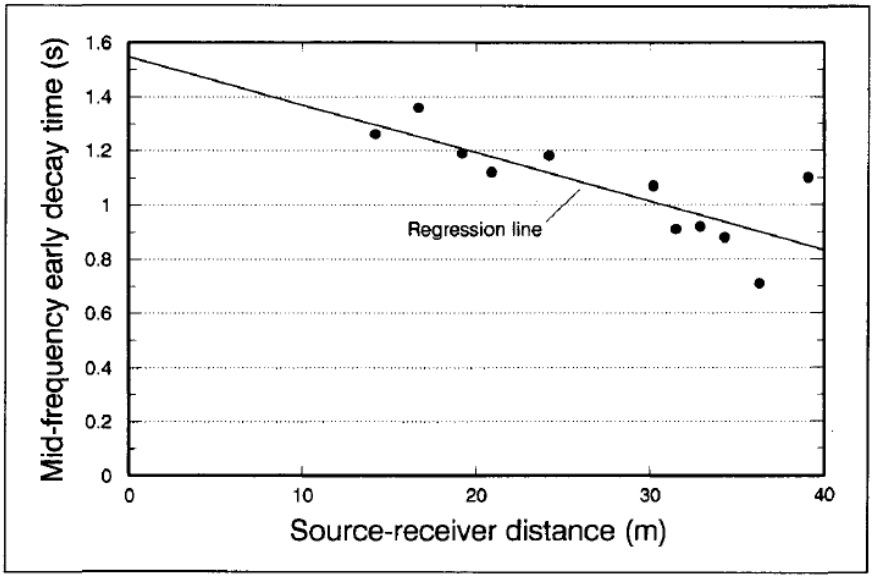


Figure 1.17: Mid frequency early decay times against source-receiver distance in one of the British concert hall [40].

positions close to the source, where the sound decay drops abruptly. It could be read as if there were problems when the expected EDT values are very short. The same author in 1996 [43] performed a round robin test and found large differences between the EDT extracted and in particular when it was short.

All the methods proposed as improvements of the Schroeder's backward integration and of the linear fitting evaluation, do not consider the specific evaluation of the EDT, neither consider the EDT as a special parameter extracted from the integrated impulse response. It is only extracted from a linear fitting made over the first part of the compensated decay. On the other hand the non-linear regression method proposed by Xiang does not consider the first 5 dB of the Schroeder's integral. Therefore, there is a strong need for a method to extract EDT in a reliable way and also on non-linearly decaying curve.

# Chapter 2

# New proposal for the decay curve extraction

The new method presented in this work is inspired to the so-called energy detection method. The energy detection method was already in use in the 50s as a demodulator. The original energy detection is based on a rectifier followed by a post detection low-pass filter [44]. The cut-off frequency of the post detection filter in this implementation was the critical point of the method. The flow chart of the modified energy detection algorithm proposed in the present work is shown in Fig.2.1.

The new proposed method proposed in this work has been called preprocessed energy detection method (EDM).

## 2.1 The new proposed method

In general the main steps to evaluate the reverberation time from a measured impulse response (IR) are:

A. the IR is filtered with an octave or one-third octave band filter (see also sec. 2.2)

B. the decay curve is extracted

C. the reverberation time is calculated with a linear fitting.

The proposed method is focused on the second step: the decay curve extraction. Here a new method is presented for the extraction of the decay curve that is intended to overcome the limits of the previous methods and improve the study of the first part of the decay.

The new proposed algorithm is composed of three main steps (see fig. 2.1):

2.1: the squared impulse response is non linearly preprocessed;

2.2: the data from step 2 are filtered with a high-slope low-pass filter;

2.3: the data from step 3 are fitted with a monotone piecewise cubic interpolation.

**Non linear preprocessing** The non linear preprocessing algorithm is an iterative algorithm and the number of iterations that gives the best performance of the method depends on the statistical characteristics of the signal and the sampling frequency. For a room impulse response, filtered or unfiltered, this number is not very critical, due to the non deterministic nature of large part of the impulse response (see fig. 2.2).

**Post-detection filter** The post detection filter returns a rough version of the envelope. In fact it is implemented, as the energy detection filter, with an high slope low pass filter. As well as the number of iterations, also the shape of the filter seems dependent on the statistical characteristics of the signal [44].

The filtered signal is processed to extract a first selection of maxima corresponding to the main maxima of the decay. It is evident that a relevant characteristics is the cut-off frequency of the filter. The filter used here has the cut-off frequency dependent on the center frequency of the octave band; so for each octave band or one third octave band the cut-off frequency of the post detection filter is different.

**Cubic interpolation** To obtain a good evaluation of the reverberation time through a linear fitting performed over the decay curve, one important feature of the decay is the monotonicity. On the other hand a good evaluation of the interpolation curve is necessary.

In 1980 Fritsch [45] proposed a new algorithm performing a monotone piecewise cubic interpolation. In the algorithm, given the monotone data values ($f_i$) at the partition points (*knots*) of the interval $I$, the goal is to construct a piecewise cubic function $p(x)$ such that $p(x_i) = f_i$ and $p(x)$ is monotone. In each sub interval $I = [x_i, x_{i+1}]$, $p(x)$ is a cubic polynomial given by

$$p(x) = f_i H_1(x) + f_{i+1} H_2(x) + d_i H_3(x) + d_{i+1} H_4(x) \tag{2.1}$$

where $d_j = p'(x_j)$ and the $H_k(x)$ are the usual cubic Hermite basis functions for the interval $I_i$. Imposing the monotonicity on a single interval and at the *knots*, a monotone piecewise cubic interpolation is obtained.

In this work this algorithm is used. Our interval is the entire impulse response, the subinterval lies between two consecutive maxima and all the maxima are the data values at the partition points. To ensure the monotonicity at the *knots*, a preliminary selection of the maxima obtained from the previous step is made.

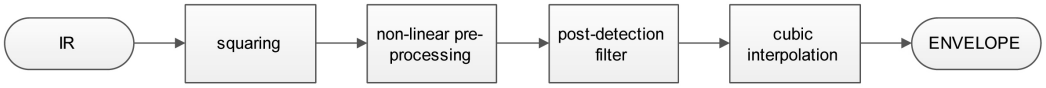


Figure 2.1: Flow chart of the proposed energy detection method (EDM) for the evaluation of the envelope of the impulse response.

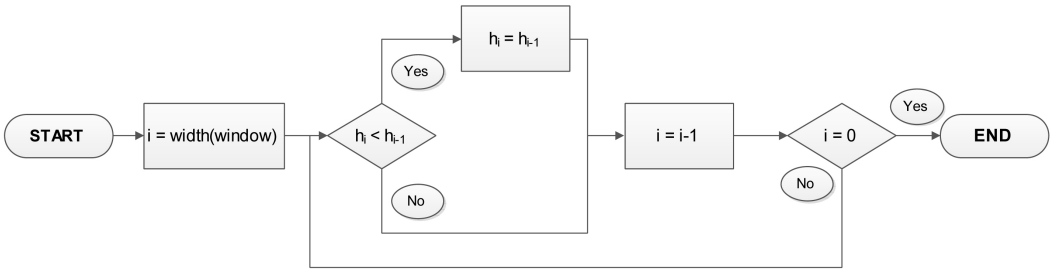


Figure 2.2: Flow chart of one iteration of the non linear preprocessing step (second step in figure 2.1).

## 2.2 Direct and reverse octave band filtering

The error due to the phase response of the digital filters on acoustics decay measurements is analysed. In literature, several works evaluate the differences between the results obtained with the direct and the reverse octave band filters. Jacobsen in 1987 [46] remarked the influence of the octave band filter on acoustic decay measurements. Through experimental analyses, he found that the influence of the filter can be considered negligible if $BT > 16$ where $B$ is the bandwidth and $T$ is the reverberation time. It is evident that the problem occurs at low frequency bands with short reverberation times and expecially performing one third octave band analyses. If the initial part of the decay is needed, a stronger condition must be satisfied that is $BT > 64$. To overcome these limits, Jacobsen and Rindel in 1987 [47] proposed the use of a time reversed filter for octave band filtering; it relaxes the condition to $BT > 4$. Later Kob and Vorländer [48] performed some computer simulation to investigate the problem. In particular they tried to detect the dependence of the error in the estimation of the reverberation time on the position of the resonance of the system under test related to the center frequency of the band. Sobreira-Seoane, Cabo and Jacobsen in 2012 [49] investigated the error due to the group delay of the filter and found that the time-reversed IIR filters show minimum distorsion. In fact using these filters, the error due to the magnitude response of the filter is counterbalanced by the error due to the phase distorsion. In 2013, the same authors [50] performed a Monte Carlo simulation, confirming the same conclusion and underlined that the time-reverse filtering advantage are limited to the estimation of the acoustic decay when the first 5 $dB$ have been discarded. In fact all the filters show large errors on the estimation of the initial part of the decay (i.e. EDT).

In this work we started from the Kob and Vorländer [48] proposal of the model impulse response

$$h_{model} = \sum_{i=1}^{n} A_i \cos(2\pi f_i t + \varphi_i) e^{\frac{-3ln10}{T_i} t} \tag{2.2}$$

which represents an acoustic system with $n$ eigenmodes each with amplitude $A_i$, frequency $f_i$ and reverberation time $T_i$. We evaluated the main three kinds of filter proposed in literature (direct IIR filter, time-reversed IIR filter and zero phase IIR filter) expecting to find the same conclusions as in the literature and thus to validate our filter.

In figure 2.3 it is presented a model impulse response of a system with five discrete modes within the one-third octave band with center frequency 63 $Hz$ and the decay curve obtained by the backward integration method as in previous literature.

In figure 2.4 different decays are compared, changing the value of the input reverberation time of the model impulse response and the octave band filter. Fig-

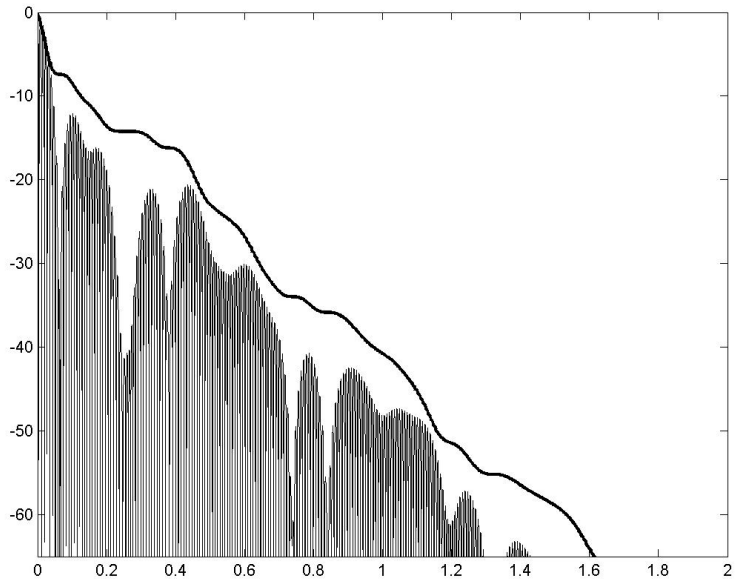


Figure 2.3: Model impulse response of a system with discrete modes. The black thick line represents the decay curve.

ures 2.4a 2.4e 2.4i show the model impulse response in the three cases: the first with a reverberation time that gives $BT > 16$, the second gives $4 < BT < 16$ and the third $BT < 4$. For each of this model impulse responses, all the three filters are tested. Table 2.1 contains the values of the relative reverberation time $T_{30}$.

The results show that the used time-reversed IIR filter gives a good evaluation of the reverberation time as found in literature. Given this, in the present work the time-reversed IIR filter is used.

Table 2.1: Values of the reverberation time $T_{30}$ calculated with three types of filter for different BT values.

| | $T_{30}$ input | $T_{30}$ direct | $T_{30}$ reverse | $T_{30}$ zero phase |
|---|---|---|---|---|
| $BT > 16$ | 1,55 | 1,70 | 1,66 | 1,75 |
| $4 < BT < 16$ | 0,43 | 0,72 | 0,61 | 0,72 |
| $BT < 4$ | 0,22 | 0,75 | 0,27 | 0,71 |

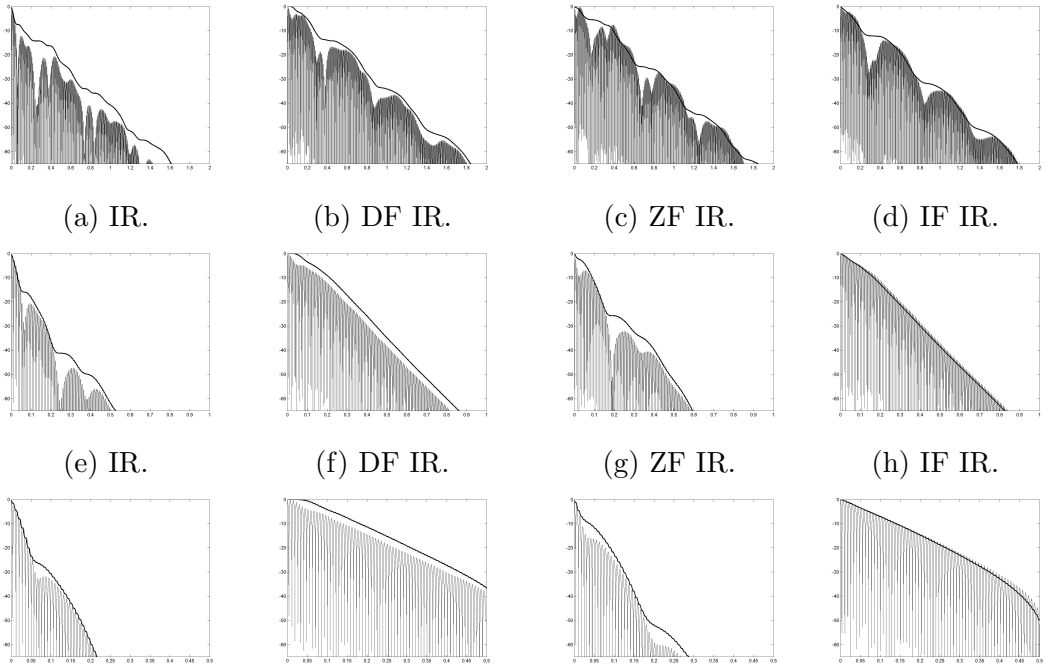

(a) IR. (b) DF IR. (c) ZF IR. (d) IF IR.

(e) IR. (f) DF IR. (g) ZF IR. (h) IF IR.

(i) IR. (j) DF IR. (k) ZF IR. (l) IF IR.

Figure 2.4: Model impulse response of a system with discrete modes in one band. Black thick line: Schroeder's backward integral. DF: direct filtering. ZF: zero phase filtering. IF: inverse filtering. First line: $BT > 16$. Second line: $4 < BT < 16$. Third line: $BT < 4$.

## 2.3 Validation of the method

Different benchmarks have been proposed to test different extraction methods [2, 51]. Some test signals in these benchmarks are synthesized using a negative exponential shaped white noise. Other tests use impulse responses measured in real rooms. It's well known that a real impulse response may be split into two regions: the early reflections, in which the acoustic field may be assumed deterministic and multimodal, and the late reverberation, in which the acoustic field may be assumed gaussian and mono modal. The two regions have a temporal split point, the so called 'mixing time' in the theory of the reverberation, that in the real IRs corresponds to a point in the decay curve located above the -5 dB point. In the case of synthesized IRs, this point is located at the 0 dB point of the decay (the mixing time corresponds to the flight time) and so the synthesized IRs are not useful to quantify the differences between EDT and RT.

In order to evaluate the performance of the proposed method, a test IR freely available has been used [2]. This real IR was used in a round robin test in 2004. From the octave band filtered IR, three different decay curves have been extracted from:

A. The method proposed in the present work (EDM)

B. The compensated Schroeder's method, using the best performing method studied by Guski and Vorländer [52, 26] with the coded present in ITA toolbox [53]

C. The bayesian method proposed by Xiang

In fig. 2.5 the three decays at 125 Hz and 1 KHz are shown.

A second order Xiang method was used, that returns two different slopes. Due to its nature, the Xiang method returns a number of decay rates related to the order of the method; each decay rate extracted represents a different decay dB-range depending on the nature of the impulse response under test. For this reason it is difficult to compare numerically the results obtained with the Xiang's bayesian method to the others.

From the decay curves, three criteria from ISO 3382 are used to quantify the reverberation time: EDT, $T_{15}$, $T_{30}$. The EDT allows to quantify the differences in the first part of the decay curve, corresponding for about half of the fitted range to the early reflections. The $T_{15}$ and $T_{30}$ allow to quantify the part of the decay curve in which the acoustic field is diffused. In the latter case, the envelope extracted with the new method and the decay curve extracted with the Schroeder's method may be assumed coincident. The method proposed in this work is here compared with the best method analysed in recent studies [52, 26], in order to

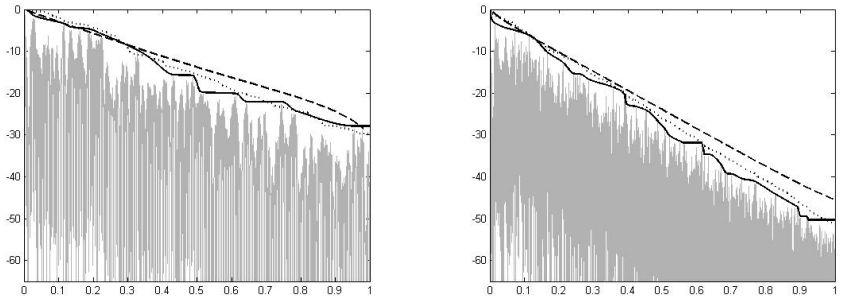

(a) IR filtered at 125 Hz octave band.

(b) IR filtered at 1000 Hz octave band.

Figure 2.5: Comparison of the three main methods for the extraction of the energy decay curve. Grey curve: filtered test impulse response. Black thick line: pre-processed energy detection method EDC. Dotted line: compensated Schroeder's integration method EDC. Dashed line: Bayesian non linear method EDC.

verify its robustness. Figure 2.6 shows the test impulse response filtered in the octave bands from $63\,Hz$ to $8000\,Hz$ with the decay curves obtained with the proposed method (thick line) and the Subtraction Truncation and Compensation improvement of the Schroeder's backward integration (dotted line). In table 2.2 the results of the Schroeder's compensated method [52, 26] are compared with the ones extracted with the present method, using the three criteria from ISO 3382.

## 2.4 Discussion of results

The comparison between the two extraction methods underlines that both return a comparable value of the reverberation time calculated over $30\,dB$ ($T_{30}$). Decreasing the range of evaluation, the two methods reveal increasing differences; in particular the main differences are in the first part of the decay (EDT). As shown in figure 2.6 the new proposed method returns a more detailed decay curve and is sensitive to each variation of the decay. On the other hand the Schroeder's integral is natively smoothed and due to its construction, is less sensitive to variations occurring at the end of the integral, that is the first part of the decay. These aspects are well represented in the numerical results (tab. 2.2) and in the figures (fig. 2.6).

The smoothness of the Schroeder's integral in general returns EDT values not so different from the reverberation time values, while in general with the new proposed method the values of EDT are very different from the relative reverberation time. Considering that the EDT value is determined by the first reflections, while the reverberation time is in general representative of the diffuse field, this aspect of

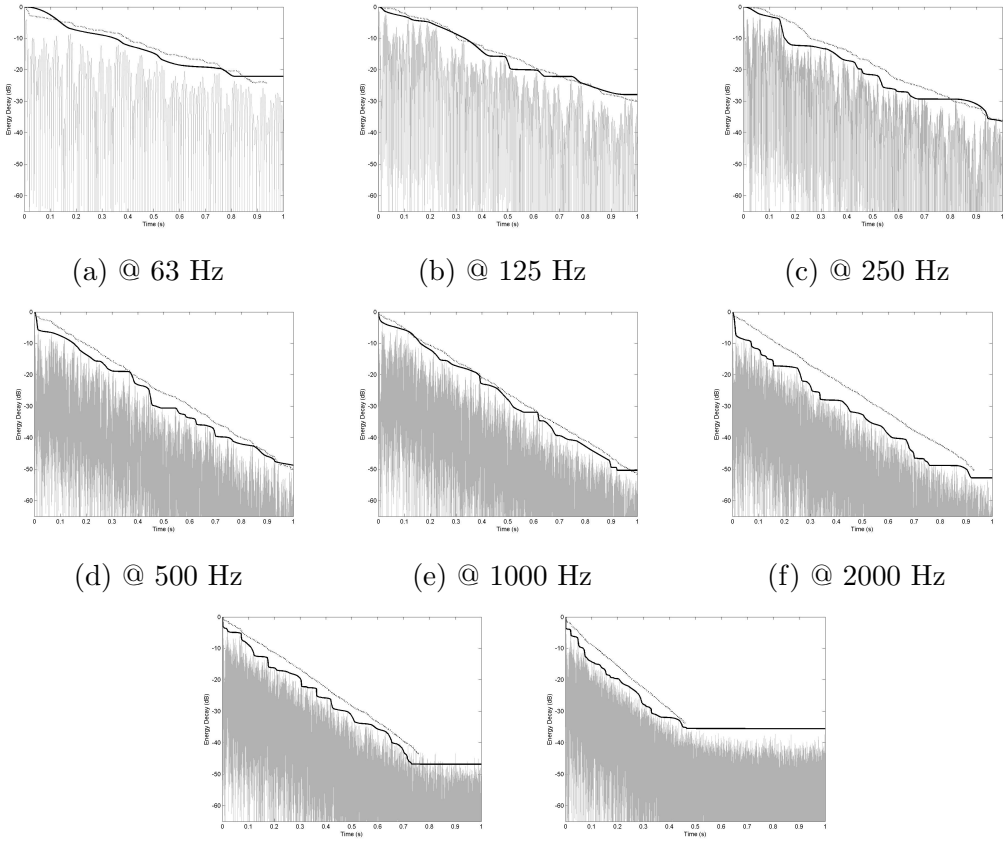

(a) @ 63 Hz (b) @ 125 Hz (c) @ 250 Hz

(d) @ 500 Hz (e) @ 1000 Hz (f) @ 2000 Hz

(g) @ 4000 Hz (h) @ 8000 Hz

Figure 2.6: Comparison of the two main methods for the extraction of the energy decay curve. Grey curve: filtered test impulse response. Black thick line: pre-processed energy detection method EDC. Dotted line: compensated Schroeder's integration method EDC.

Table 2.2: Reverberation time values calculated for the test signal.

| Octave band | Criterion | Compensated Schroeder | New method (EDM) |
|---|---|---|---|
| 63 Hz | EDT (s) | 3.09 | 1.88 |
| | $T_{15}$ (s) | 2.45 | 2.36 |
| | $T_{30}$(s) | — | — |
| 125 Hz | EDT (s) | 2.16 | 2.19 |
| | $T_{15}$ (s) | 1.72 | 1.37 |
| | $T_{30}$(s) | 1.98 | — |
| 250 Hz | EDT (s) | 1.65 | 1.54 |
| | $T_{15}$ (s) | 1.56 | 2.03 |
| | $T_{30}$(s) | 1.61 | 1.90 |
| 500 Hz | EDT (s) | 1.24 | 0.94 |
| | $T_{15}$ (s) | 1.17 | 1.31 |
| | $T_{30}$(s) | 1.21 | 1.16 |
| 1 KHz | EDT (s) | 1.12 | 1.19 |
| | $T_{15}$ (s) | 1.23 | 1.17 |
| | $T_{30}$(s) | 1.17 | 1.13 |
| 2 KHz | EDT (s) | 1.11 | 0.37 |
| | $T_{15}$ (s) | 1.12 | 1.04 |
| | $T_{30}$(s) | 1.15 | 1.05 |
| 4 KHz | EDT (s) | 1.07 | 0.76 |
| | $T_{15}$ (s) | 1.13 | 1.06 |
| | $T_{30}$(s) | 1.09 | 1.09 |
| 8 KHz | EDT (s) | 0.74 | 0.40 |
| | $T_{15}$ (s) | 0.87 | 0.74 |
| | $T_{30}$(s) | — | 0.87 |

the new proposed method could be considered a good characteristics.

# Part II

# Experimental Results

# Chapter 3

# Measurements in Italian historical theatres

In this chapter the results of the measurements performed in nine Italian historical theatres are presented.

The analysis performed on theatres has the advantage that in some way could be compared with the studies of Barron [40] in concert halls and in particular with those works focused on the importance of the evaluation of the EDT as explained in sections 1.5 and 1.6. In this chapter the results obtained from the new proposed method *preprocessed energy detection method (EDM)* applied on the impulse responses measured in each theatre are presented. Then the results are compared with the results of reverberation time and EDT obtained with the compensated Schroeder's backward integration method.

As shown in section 2.3 and underlined in section 2.4, with the energy detection method a different evaluation made on the first part of the decay is expected and in particular a different EDT value is expected due to the ability of the new proposed method to return a more detailed energy decay curve.

## 3.1 The Italian historical theatre

The Italian historical opera house is an architectural typology that dates back to the XVII century. The milestone of this this family of theatres is the Farnese Theatre in Parma, which introduced many typological features - e.g. the proscenium arch - that characterize the Italian historical opera house since then.

In this period the first essays on the Italian theatre started to appear, two among all the Carini Motta (1676) and the Milizia (1771) ones. The optimal plan shape of the theatre is widely discussed in these essays, and each author has his preference that varies between semi-elliptical, semicircular, U shape, bell shape

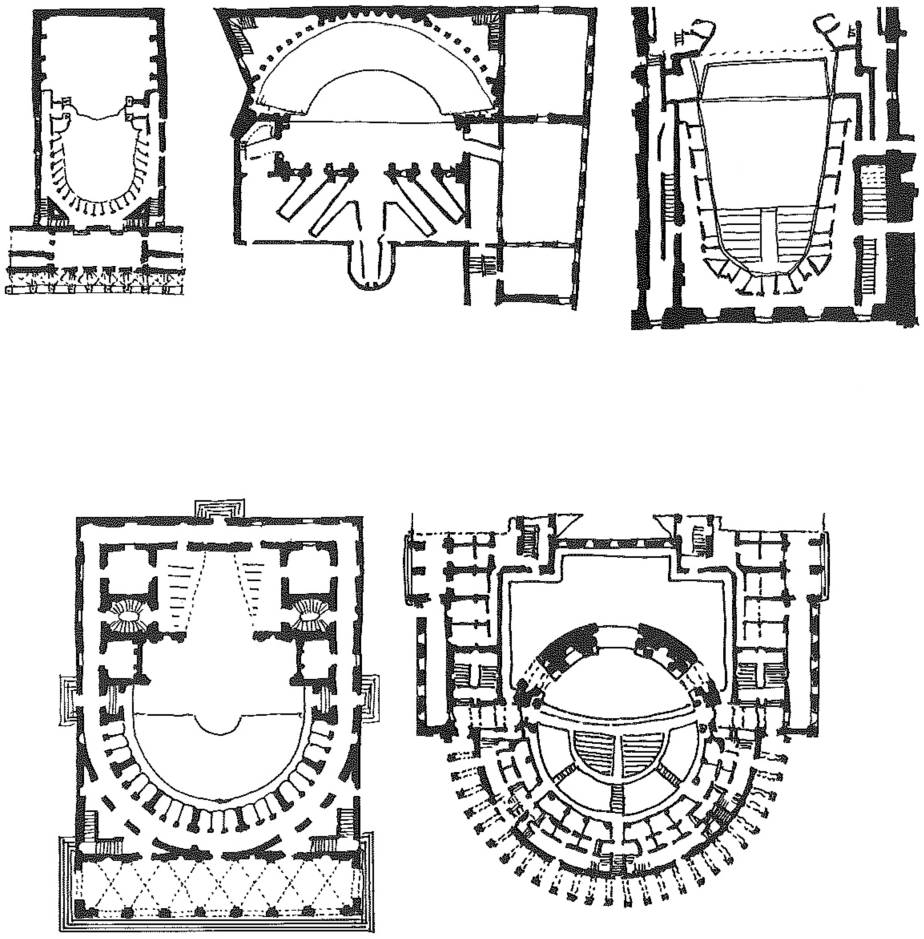

Figure 3.1: Typical plan schemes [54].

and, finally, horseshoe shape.

Typical plan schemes are shown in figure 3.1. From the left:

A. horseshoe shape of the Bologna Town Theatre (1756, architect Galli Bibiena);

B. semielliptical shape of the Vicenza Theatre (1580, architects Palladio and Scamozzi);

C. open U shape of the Molière hall at the Palais Royal in Paris (1640);

D. project of a semicircular shape (1762, architects Arnaldi);

E. project of a circular shape (1771, architect Ferrarese).

The main characteristics that distinguish the Italian opera house is the presence of different coupled volumes. In particular, the theatre is made up by two main volumes: the stage house, in which the scenes are moved, and the volume in which the audience stay, which will be referred to as cavea. The cavea itself is surrounded by smaller volumes, i.e. the boxes. The stage house and the cavea are connected via the proscenium arch, which plays a key role dealing with first reflections. In particular, its presence enhances the reflections coming from the sound source, both if the source is positioned in the front of the stage (typical position for singers) and if it's placed in the rear part of the stage. Between the stage house and the main hall lies also the orchestra pit, which was often added to the original architecture of the theatre, being its existence made fundamental after the Wagner's experience. Often, the lowest area of the cavea is covered by a marmorino plaster for a height of about 2 m from the ground. It is a very smooth plaster made of slaked lime and marble dust which provides very strong reflections with little attenuation, and is determinant for the sound field in the audience. The structure of the theatre is mainly made of light-weighting wood structures. In particular, the wood structure of the stage and the stalls floor provide interesting contributions to the sound field in terms of coloring. Another critical structure is the vault, which is realized with the arellato technique. This technique was used to cover wide areas with light-weighing structures. It basically consists of a wood structure to which reed mats are fixed; then a fresco usually finishes the work. Also the vault, nearly flat, provides important first reflections to the rear part of the audience when the source position is frontal.

The distinctive feature of the Italian opera house is a very good clarity of sound. Since the shape of the theatre is optimized for the opera, the listener must be able to distinguish clearly the words of the singer, feature which is not essential for symphonic music, in which the blending of sounds is absolutely necessary. Acoustically speaking, all the architectural features mentioned above have a great correspondence with the acoustical need of clarity. The Italian historical opera

house is a balanced mix of highly reflective and highly absorptive surfaces which are combined to provide a unique listening experience. In particular, four of these are: the presence of coupled volumes, which provide the typical cliff-type decay, the proscenium arch, which separates the two coupled volumes and enhances the first reflections, the vault and the marmorino surface, with their important contribution in terms of first reflections. The acoustic criteria most deeply influenced by these features are the ones strongly depending on first reflections, i.e. EDT and $C_{80}$.

## 3.2 The measured halls

The Interdepartmental Center for Industrial Research (CIRI) funded the project "Historical theatres of Emilia-Romagna" (table 3.1), which so far led to perform acoustic measurements in 12 historical opera houses in Northern of Italy. The theatres under study have different features but were built within a period of 100 years in the same geographical and political context. The size varies from small to medium theatres. The shape of some of them are resumed in the following figure 3.3. It can be clearly seen that, though the overall conception is common to all theatres, many features differ non only by a scaling factor (tab. 3.2).

For each theatre the measurements were performed with different source positions and for at least of one of these source position all seats were measured. In general, monaural impulse responses were recorded for each listening position in the audience, at least one position in each box and one position for each seat in the gallery. This permits to have a complete characterization of the theatre and with this set of measurements it is possible to evaluate each specific behaviour of the theatre. Due to the particular typology of these theatres, the complete set of measurements can also be considered heterogeneous.

### 3.2.1 Differences with the theatres measured by Barron

The Italian historical theatre differs strongly from the concert hall typology. This is mainly due to the need - for the performance of the opera - to have two separated volumes, one for the audience and one for the stage and the scenes. Then, as remarked before, the Italian historical theatre is devoted to opera, which is a genre that requires good intelligibility and low reverberation time compared to halls designed for symphonic music. In particular, the halls analysed by Barron present architectural and acoustical features which can be resumed as follows. The volumes of the theatres are greater than those typical of Italian historical opera houses (for which a doubt arises: which volume shall be considered?). The halls dimensions imply high values of ITDG, on the contrary of what happens in Italian historical theatres in which very strong first reflections with low values of ITDG

Table 3.1: The measured theatres: name, location and tag.

| Location | Name | Tag |
|---|---|---|
| Cesena | Bonci Theatre | BON |
| Faenza | Masini Theatre | MAS |
| Lugo | Rossini Theatre | ROS |
| Imola | Stignani Theatre | STI |
| Meldola | Dragoni Theatre | MEL |
| Cesenatico | City theatre of Cesenatico | CES |
| Russi | City theatre of Russi | RUS |
| Cervia | City theatre of Cervia | CER |
| Longiano | Petrella Theatre | LON |

Table 3.2: The measured theatres: shape, volume and seat capacity.

| | Typology | Volume of the cavea | Volume of the stage | Mean volume of boxes | Number of seats | Order of boxes |
|---|---|---|---|---|---|---|
| BON | horseshoe | 2798 $m^3$ | 10282 $m^3$ | 9 $m^3$ | 800 | 4 |
| MAS | horseshoe | 2628 $m^3$ | 3034 $m^3$ | 6 $m^3$ | 500 | 4 |
| ROS | elliptic | 1455 $m^3$ | 2392 $m^3$ | 5 $m^3$ | 448 | 4 |
| STI | horseshoe | 1752 $m^3$ | 1523 $m^3$ | 5 $m^3$ | 468 | 3 |
| MEL | horseshoe | 1205 $m^3$ | 880 $m^3$ | 10 $m^3$ | 318 | 3 |
| CES | horseshoe | 733 $m^3$ | 1024 $m^3$ | 9 $m^3$ | 271 | 2 |
| RUS | horseshoe | 924 $m^3$ | 755 $m^3$ | 7 $m^3$ | 305 | 2 |
| CER | horseshoe | 858 $m^3$ | 630 $m^3$ | 7 $m^3$ | 224 | 2 |
| LON | horseshoe | 697 $m^3$ | 1251 $m^3$ | 8 $m^3$ | 241 | 2 |

(a) Bonci Theatre

(b) Masini Theatre

(c) Rossini Theatre

(d) Stignani Theatre

(e) Dragoni Theatre

(f) Cesenatico Theatre

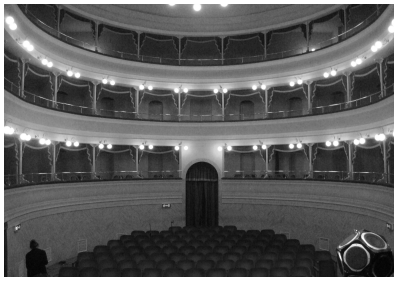

(g) Russi Theatre

(h) Cervia Theatre

(i) Petrella Theatre

Figure 3.2: Photos of the measured Italian historical theatres.

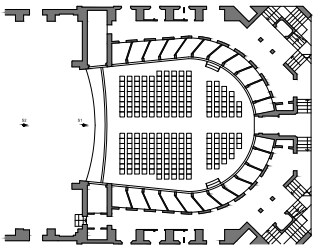

(a) Bonci Theatre

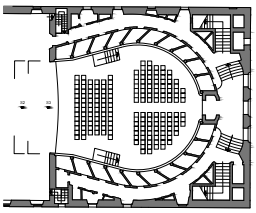

(b) Masini Theatre

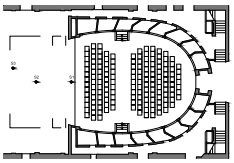

(c) Rossini Theatre

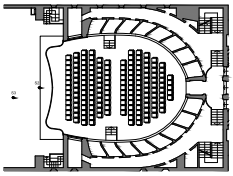

(d) Stignani Theatre

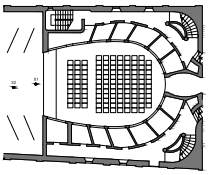

(e) Dragoni Theatre

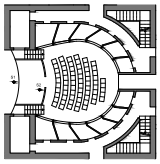

(f) Cesenatico Theatre

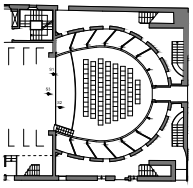

(g) Russi Theatre (0)

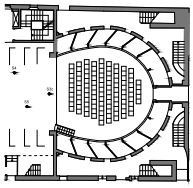

(h) Russi Theatre (C)

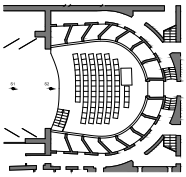

(i) Cervia Theatre

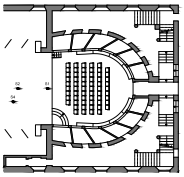

(j) Petrella Theatre

Figure 3.3: Scaled plans of the measured Italian historical theatres.

are found. This is due mainly to the already mentioned geometrical characteristics.

## 3.3 Main results

The measurements performed in each theatre have been post-processed and for each impulse response the monaural acoustic parameters have been extracted. In particular, from each measured impulse response the early decay time value and the reverberation time $T_{30}$ value have been extracted using the new proposed method for the evaluation of the decay curve.

For a more detailed analysis, each extracted criterion has been represented in a graphical form through the interpolation of the values over the whole area (e.g. the stalls area). It is important to note that the interpolation was only useful for a graphical scope: the amount of interpolation points (the measured positions) is so large that it is possible to affirm that the interpolation procedure cannot create any artefact in the final representation.

For example, in figures 3.4 and 3.5 the results are presented for EDT and $T_{30}$ extracted from the impulse responses measured in the audience of the Bonci theatre in Cesena with both the sound source positions.

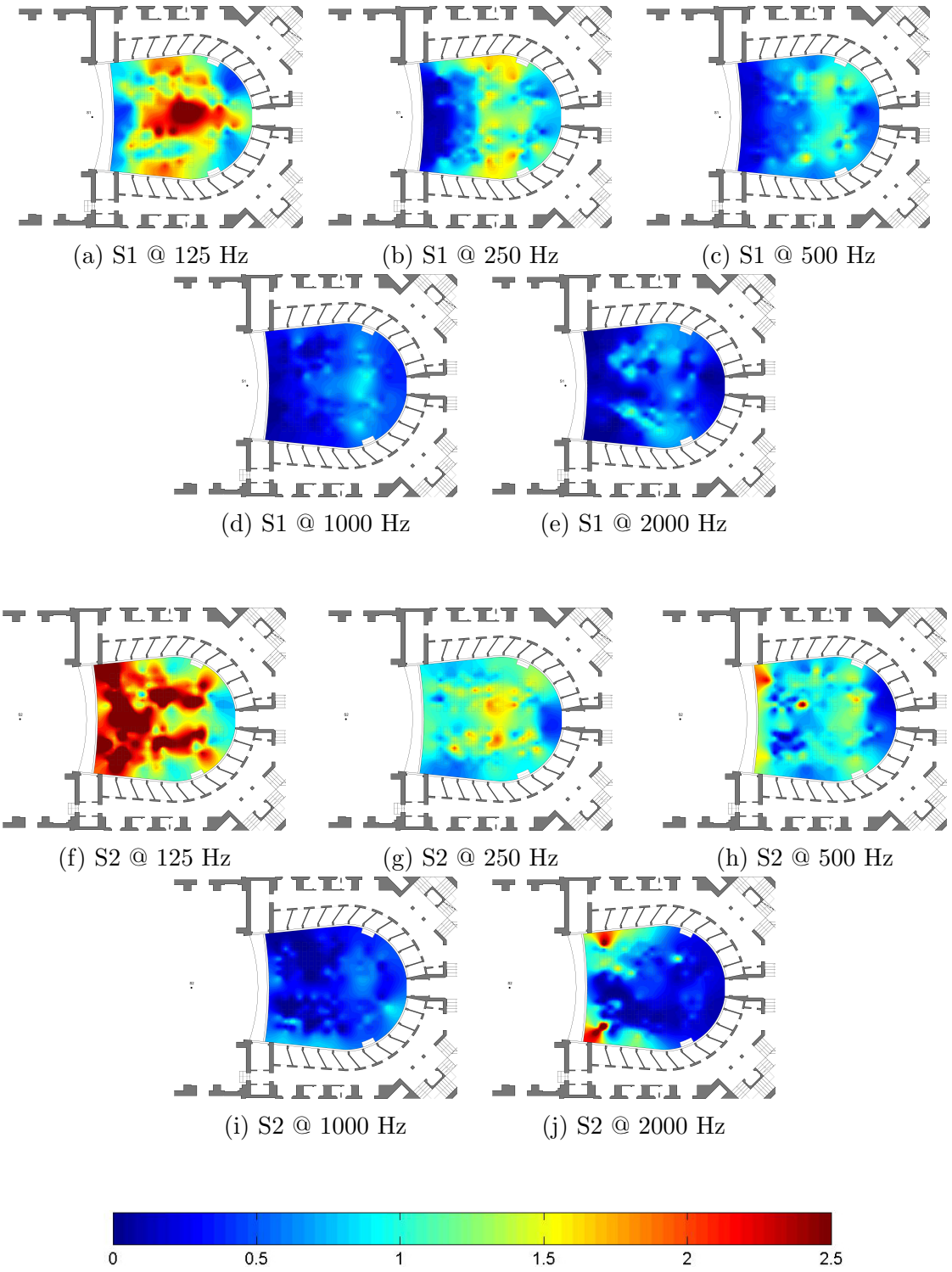


(a) S1 @ 125 Hz (b) S1 @ 250 Hz (c) S1 @ 500 Hz

(d) S1 @ 1000 Hz (e) S1 @ 2000 Hz

(f) S2 @ 125 Hz (g) S2 @ 250 Hz (h) S2 @ 500 Hz

(i) S2 @ 1000 Hz (j) S2 @ 2000 Hz

Figure 3.4: Interpolation maps of the EDT measured in the audience of the Bonci theatre for both the sound source positions.

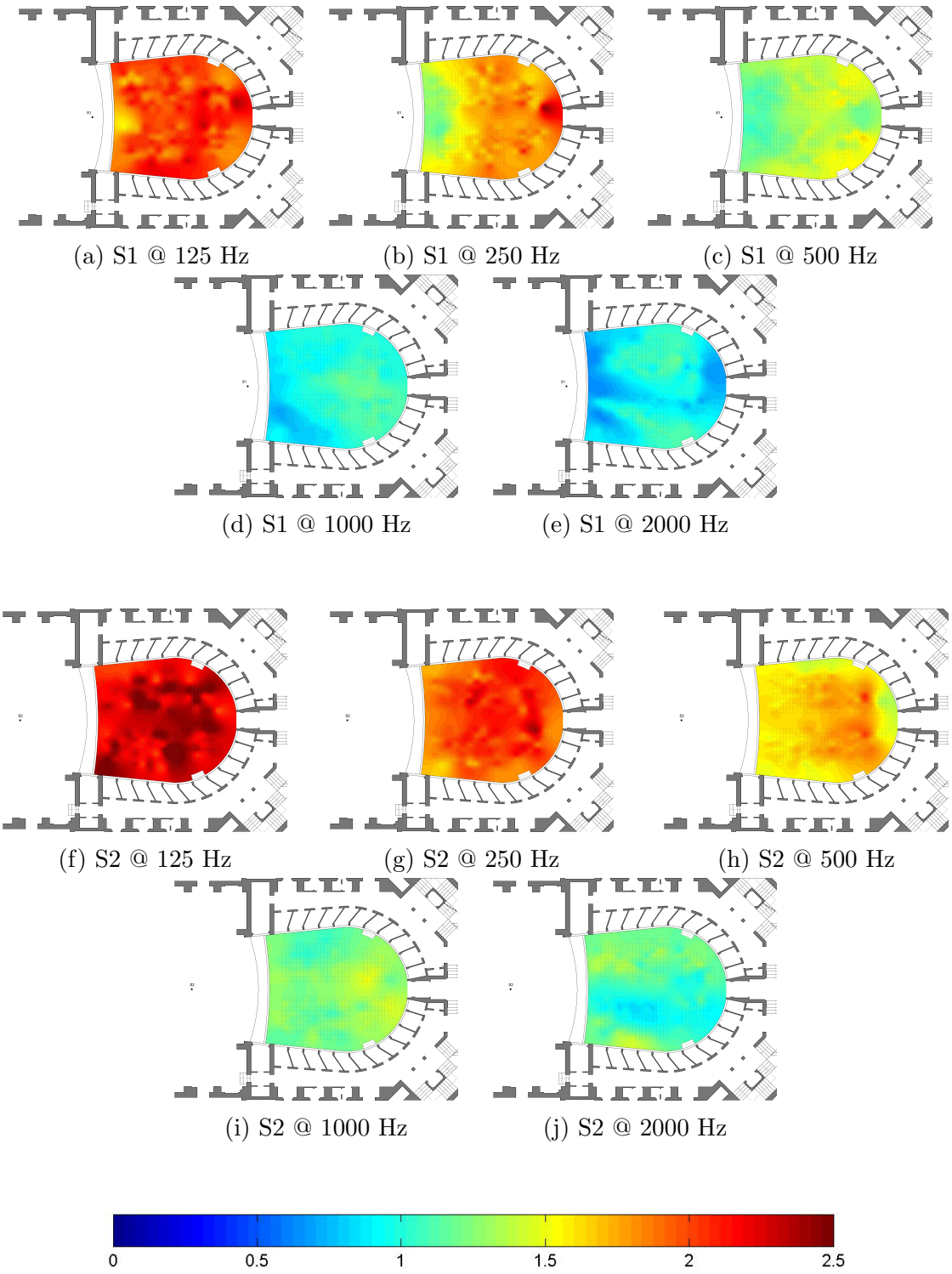


(a) S1 @ 125 Hz (b) S1 @ 250 Hz (c) S1 @ 500 Hz

(d) S1 @ 1000 Hz (e) S1 @ 2000 Hz

(f) S2 @ 125 Hz (g) S2 @ 250 Hz (h) S2 @ 500 Hz

(i) S2 @ 1000 Hz (j) S2 @ 2000 Hz

Figure 3.5: Interpolation maps of the $T_{30}$ measured in the audience of the Bonci theatre for both the sound source positions.

## 3.4 Considerations

As previously explained, the main feature of the new proposed method could be found in its ability to catch the single variations on the envelope of the decay. For this reason the most interesting considerations could be focused on the first part of the decay, the one with more local variability. The considerations about the reverberation time will be made in section 3.5 as a comparison with the literature methods.

The maps related to the evaluation of EDT in the audience show that the values of the criterion have a wide distribution. That was an expected behaviour due to capability of the new proposed method to return a detailed decay curve that in terms of EDT could be read as a spread distribution of values. To analyse the validity of the results related to the real decay in the impulse response, here some evaluations of EDT values with the relative impulse responses are presented.

For example in figure 3.6 the maps of EDT are shown in the octave band with center frequency $125\,Hz$ with two source positions. In order to compare the two maps in figures 3.6a and 3.6e, three positions in the audience are chosen; one in the front on the right (listening position number 16) and two in the center of the audience (listening positions number 118 and 154). The EDT evaluated in the center of the audience at position 118 shows high values independently of the source position, while for the other two seats the EDT assumes different values depending on the source position.

The relative impulse responses shown in the corresponding subfigures of figure 3.6, reveal that this evaluation directly corresponds to the distribution of reflections and that the energy detection method detects these differences.

(a) S1 EDT. (b) S1 Pos.#16 (c) S1 Pos.#118 (d) S1 Pos.#154

(e) S2 EDT. (f) S2 Pos.#16 (g) S2 Pos.#118 (h) S2 Pos.#154

Figure 3.6: Analysis of the impulse response corresponding to particular values in the interpolation maps of the EDT at 125 Hz extracted with the pre-processed energy detection method. Location of position#16: front right. Location of positions #118 and #154: center.

## 3.5 Comparison with literature methods

To compare the new proposed method with the compensated Schroeder's backward integration method, here the evaluation of the same impulse responses measured in the audience that have been discussed in section 3.4 is presented (fig. 3.7). In this case the EDT values, expecially in case of the measurements performed with the source position S1, seem to be less sparse compared with the same values extracted with the new proposed method. Also the values extracted for the source position S2 have the same characteristics: here in particular it is possible to note that there are no differences between listening positions number 118 and 154, as it was in figure 3.6.

Focusing the attention on the impulse responses in figure 3.7 it is possible to note that in this case the energy decay curves are smooth and do not depend on the local changes of the decay. The differences between EDT values extracted with the energy detection method for source positions S1 and S2 (fig. 3.6) are due to the dependence of the energy decay curves exactly on this fact.

For a complete comparison of the two methods, an evaluation of the reverberation time $T_{30}$ values is also needed. On one hand it is expected that the two methods match and return similar values for low frequencies, while for high frequencies there could be some differences: at high frequencies the slope of the decay increases and the characteristics of the new method of no 'delay' in the response could become useful.

Figures 3.8 and 3.9 show the values of reverberation time $T_{30}$ extracted with the compensated Schroeder's backward integration method (in the first line of each figure) and with the new proposed method (in the second one) for both the source positions. In the third line an example of impulse response is shown filtered in the relative octave bands with both the energy decay curves.

(a) S1 EDT. (b) S1 Pos.#16 (c) S1 Pos.#118 (d) S1 Pos.#154

(e) S2 EDT. (f) S2 Pos.#16 (g) S2 Pos.#118 (h) S2 Pos.#154

Figure 3.7: Analysis of the impulse response corresponding to particular values in the interpolation maps of the EDT at 125 Hz extracted with the compensated Schroeder's integration method. Location of position#16: front right. Location of positions #118 and #154: center.

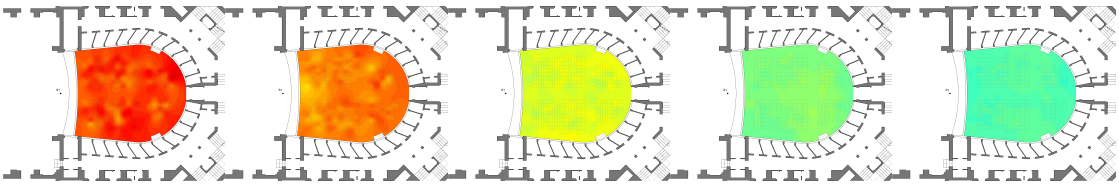

(a) @ 125 Hz (b) @ 250 Hz (c) @ 500 Hz (d) @ 1000 Hz (e) @ 2000 Hz

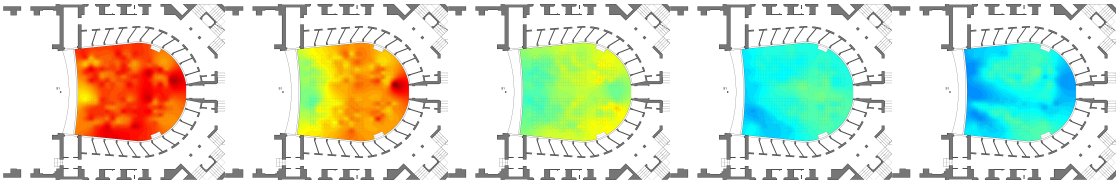

(f) @ 125 Hz (g) @ 250 Hz (h) @ 500 Hz (i) @ 1000 Hz (j) @ 2000 Hz

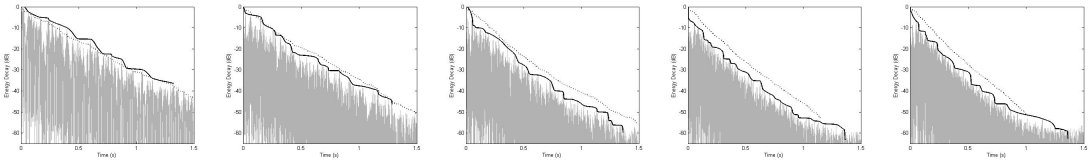

(k) IR @ 125 Hz (l) IR @ 250 Hz (m) IR @ 500 Hz (n) IR @ 1000 Hz (o) IR @ 2000 Hz


Figure 3.8: Comparison of interpolation maps calculated for $T_{30}$ with source position S1 with both the energy decay curve extraction methods. First line: compensated Schroeder's integration method. Second line: preprocessed energy detection method. Third line: example of impulse response measured in one of the center positions (#118).

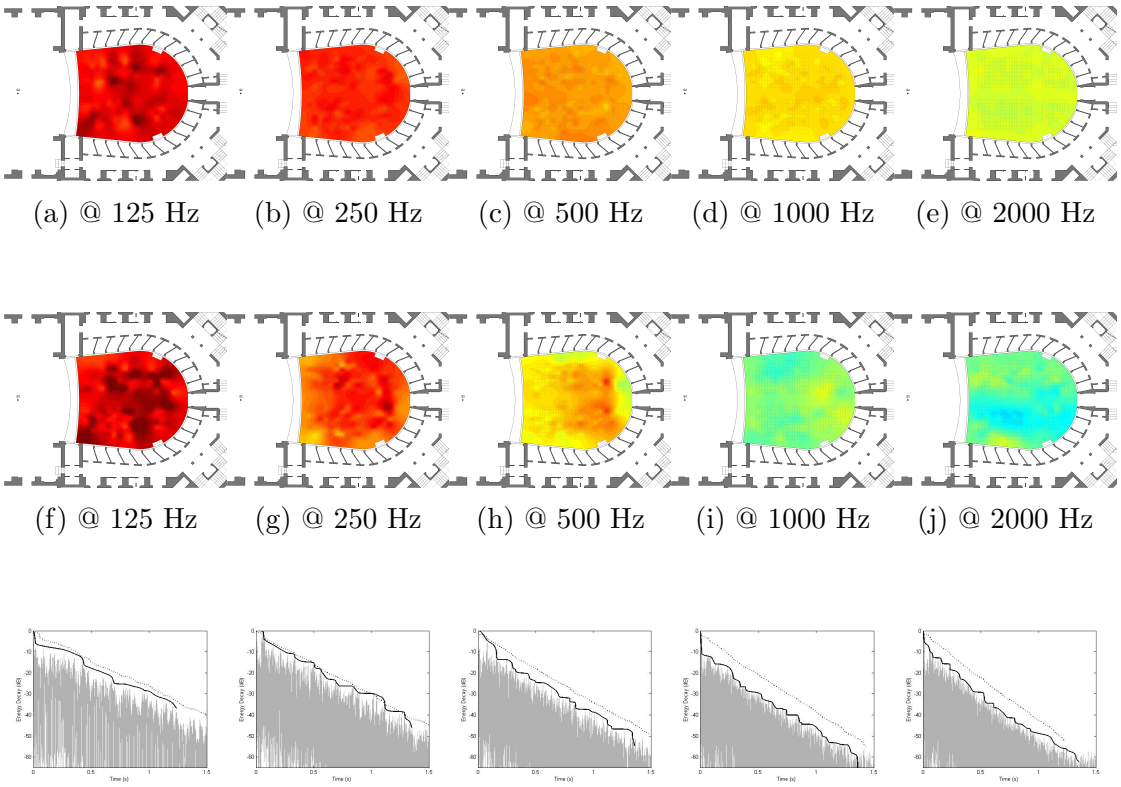


(a) @ 125 Hz (b) @ 250 Hz (c) @ 500 Hz (d) @ 1000 Hz (e) @ 2000 Hz

(f) @ 125 Hz (g) @ 250 Hz (h) @ 500 Hz (i) @ 1000 Hz (j) @ 2000 Hz

(k) IR @ 125 Hz (l) IR @ 250 Hz (m) IR @ 500 Hz (n) IR @ 1000 Hz (o) IR @ 2000 Hz

Figure 3.9: Comparison of interpolation maps calculated for $T_{30}$ with source position S2 with both the energy decay curve extraction methods. First line: compensated Schroeder's integration method. Second line: preprocessed energy detection method. Third line: example of impulse response measured in one of the center positions (#118).

## 3.6 Barron's evaluations applied to the Italian Historical Theatres

The differences between the early decay time and the reverberation time, expecially when extracted with the new proposed method, suggest that the application of the Barron's theory about EDT itself and about its relation with the measured reverberation time could be an interesting aspect to analyse. Therefore is performed a Barron like analysis has been performed on the values resulting from the energy decay curve extracted with both the compared methods.

As explained in section 1.6, the ratio between the early decay time and the reverberation time $\frac{EDT}{RT}$ could be an interesting parameter to analyse. Figure 3.10 presents the ratio calculated for all the theatres with the compensated Schroeder's backward integration method (compSCH) and with the pre-processed energy detection method (EDM). Two sound source positions are considered: one in the front of the stage, typically under the proscenium arch, and the other approximately in the middle of the stage. As in Barron's results, the evaluation is performed averaging the values of EDT and RT in the three middle octave bands from 500 Hz to 2000 Hz. In figure 3.10a, the values calculated in the Russi Theatre, have been presented for the two configurations with the opened orchestra pit (RUSSI-O) and with the closed orchestra pit (RUSSI-C). In this evaluation the results for both the orchestra pit configurations have been used separately assuming that the spatial distribution of the EDT value could be different for the two.

As shown in figure 3.10, for both source positions the values of the ratio $\frac{EDT}{RT}$ calculated with the energy detection method is significantly smaller that the one calculated with the compensated Schroeder's integration method. Considering the previous results of both the criteria, this was predictable, due to the fact that the EDT values calculated with the energy detection method are sensitively smaller than the ones calculated with the compensated Schroeder's backward integration method, while the values of the reverberation time are comparable.

It is also important to discuss the meaning of the values of the ratio $\frac{EDT}{RT}$ related to the physical characteristics of the theatres as suggested by Barron. Due to their shape, the Italian historical theatres have the characteristics to focus the reflections to the audience: this suggests that the ratio has to be less than one. For the front source, all the values for both the decay extraction methods are less than one, while for the rear source this is true only for the new extraction method.

It is also important to note that all the values extracted for these Italian historical theatres have a wide range of variation of the ratio $\frac{EDT}{RT}$ compared with the theatres analysed by Barron [40]. This is due to the peculiar shape of the Italian historical theatre and to the related feature of its architectural elements of focusing reflections. The theatres which have been measured present differences

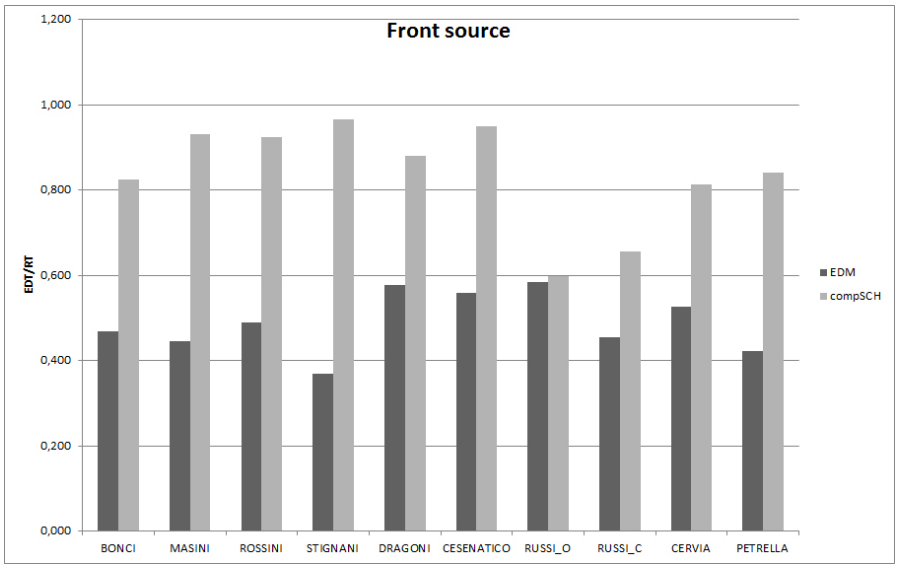


(a) Front source S1.

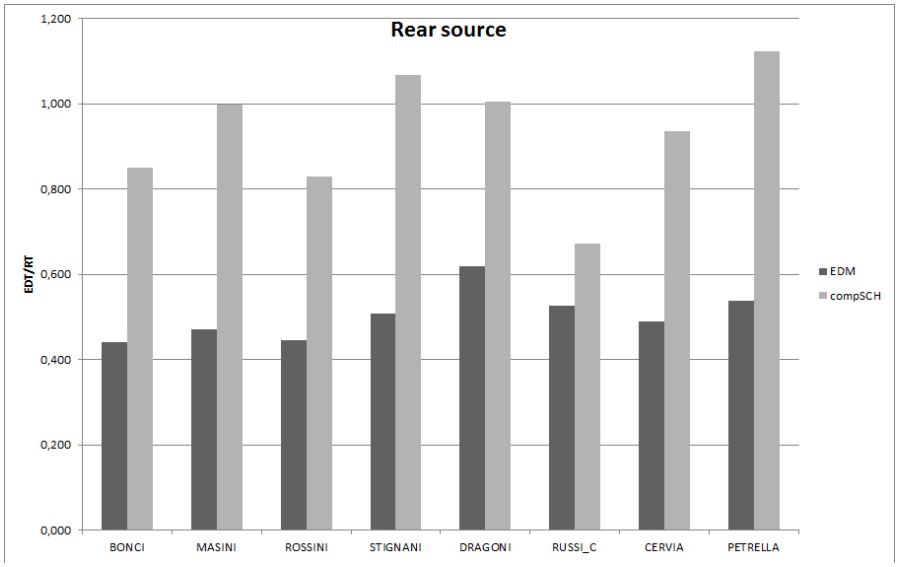


(b) Rear source S2.

Figure 3.10: EDT-RT ratio calculated with both the energy decay curve extraction methods. Light grey: compensated Schroeder's backward integration method. Dark grey: preprocessed energy detection method.

in the geometry - which do not differ only by a scaling factor - and that affect the sound field dramatically.

Among the measured theatres, one has a particular surface treatment of the lateral sides of the audience: it is the Dragoni theatre that, instead of a reflecting surface, presents a velvet covering. Considering this characteristics, the greater values of the ratio $\frac{EDT}{RT}$ for this theatre calculated with the energy detection method can be considered representative for both source positions.

Following Barron's study, also the ratio between the EDT value and the source-receiver distance gives interesting information about the acoustics of the theatres [40]. In this work the choice of representing the results with the interpolation maps on the measured position permits us to make the same kind of evaluation. Moreover, this kind of representation of results contains other information about the distribution of the values in the audience: with the interpolation maps it is possible not only to evaluate the variation of EDT related to the distance but it is possible also to identify the spatial variation of the same criterion. To compare the Barron's results with the one in the present study, the interpolation maps of the EDT are represented averaging the EDT values in the octave bands from 500 to 2000 Hz (fig. 3.11).

The Barron's evaluations return a decreasing value of EDT with distance in the region near the source and a uniform distribution far from the source. The figures show a different behaviour of EDT values in the audience of the Italian historical theatres. The two extraction methods return different distributions of the EDT. The compensated Schroeder's integration method returns values of EDT that decrease with the distance between the source and the receiver, expecially if the source considered is the rear one. Different results for the energy detection method: the values of EDT evaluated averaging the values extracted in the octave bands from 500 Hz to 2000 Hz are in general uniformly distributed in the audience, both for the front and the rear source positions. It is possible to identify only a particular region of the audience where the values of EDT are greater than in the other areas; this effect is more evident with the front source. Considering only the source positioned in the middle of the stage, also the very frontward lateral area of the audience returns values of the EDT greater than the others and this is probably due to the relative position of the proscenium related to the audience, that is another typological feature of the considered theatres.

The behaviour of the EDT values calculated from the energy decay curve extracted with the new proposed method seems to correspond to the distribution of early reflections in the audience. In fact, the architecture of the Italian historical theatres suggests that the linear distance could not be the most meaningful parameter for the evaluation. Due both to the aspect ratio and to the particular shape of the plan, the concept of distance that could be compared with the linear

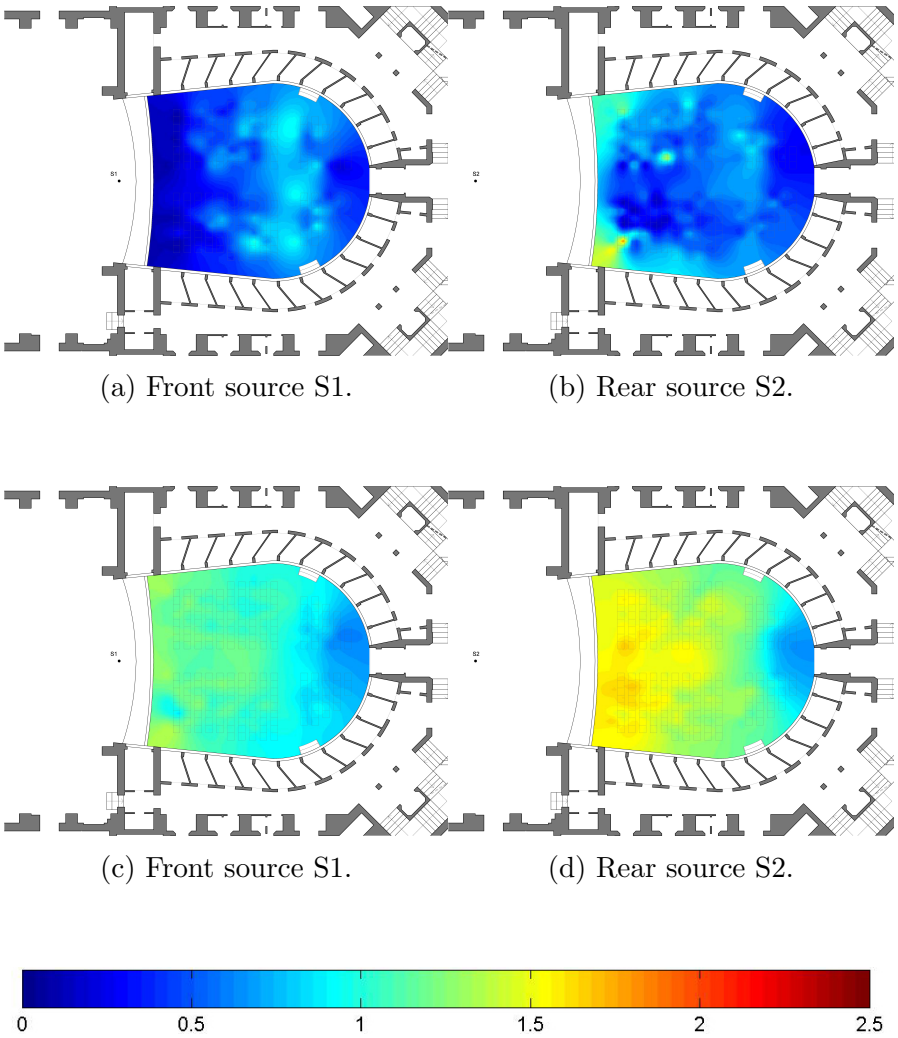


(a) Front source S1. (b) Rear source S2.

(c) Front source S1. (d) Rear source S2.

Figure 3.11: Interpolation maps of the EDT values extracted from the measurements performed in the Bonci theatre with both the energy decay curve extraction methods at mid frequency (averaged in the octave bands from 500 Hz to 2000 Hz). First line: preprocessed energy detection method. Second line: compensated Schroeder's integration method.

distance considered by Barron, could be reviewed in the sense of difference between the direct sound distance and the distance from the nearest surface.

In particular, the areas that can be considered far from the source are also near the sidewalls of the audience. Moreover the sides of the audience are typically realized with a very smooth material that enhances the reflections. In this optics the results of the EDT evaluations for the audience presented in figures 3.11a and3.11b confirm the hypothesized behaviour of the reflections.

With the new definition of the concept of distance used here, the central area where the measured EDT values are greater than in other areas, could be seen as the one with the most delayed reflections.

The new proposed method for the extraction of the energy decay curve, due to its detail, returns EDT values well correlated with the distribution of single reflections.

# Chapter 4

# Measurements in critical cases

A correct evaluation of reverberation time is very important not only in the case of acoustic characterization of performance spaces, where it is related to the acoustic quality of the space as previously described, but also in the case of building acoustics. In the case of building acoustics, the reverberation time is a widely used criterion both for laboratory and *in situ* measurements. For example, it is needed to normalize sound reduction index measurements in the laboratory and the sound difference level *in situ* [55]. Moreover the structural reverberation time of building elements is needed to calculate the structural coupling loss factor and the vibration reduction index [56, 57].

The evaluation of reverberation time calculated from structural impulse responses, could be an interesting case study for the present work. In fact, structural impulse responses present in general two particular characteristics: on one hand the decay rates are very high and the reverberation times are very short, on the other hand the useful decay ranges are very small.

Two of the main characteristics of the new proposed method, the energy detection method, are its ability to detect with no 'delay' the variation of the decay of the squared impulse response and its independence from the background noise. This suggests that the use of the new proposed method could overcome the problems related to the extraction of reverberation time from structural impulse responses.

Due to the shortness of the typical reverberation time calculated for structural impulse responses and to the fact that typically in this case the criteria have to be extracted in one third octave bands, it is important to remember the influence of the octave band filter in the evaluation: the resulting product $BT$ could assume very small values ($BT < 4$). In this case fundamental condition is not respected and both the methods can't be applied due to the limit of the filtering procedure.

To test the performances of the new proposed method for the extraction of the decay energy curve and to compare the results with literature method (the compensated Schroeder's backward integration method), two different sets of mea-

surements have been performed. Both sets of measurements have been done in the laboratory: the first is composed by impulse responses for a brick wall and the second one for a reinforced concrete slab. Although both sets maintain the typical characteristics of structural impulse response, they could return different values due to the different homogeneity of the samples. While the brick wall can be considered a heterogeneous test specimen, the concrete slab can be considered as an homogeneous one.

For the structural impulse response measurements, a hammer as impulsive source has been used. The instrumentated hammer has been used with three different tips: rubber, teflon and steel. Each of these three tips has the characteristic to excite linearly different frequency bands in the structure: the rubber excites the bands between 100 Hz to 700 Hz, the teflon the bands between 300 Hz and 1000 Hz, and the steel between 500 Hz and 5000 Hz. For each source-receiver position, three measurements have been performed, each with one of the three different tips. The final results have been composed using the response obtained with the rubber tip filtered in the one third octave bands between 100 Hz and 315 Hz, the response obtained with teflon tip filtered in the one third octave bands between 400 Hz and 630 Hz and the response obtained with the steel tip filtered in the one third octave bands between 500 Hz and 4000 Hz.

## 4.1 Comparison with literature methods

Figures 4.1 and 4.2 show the values of EDT and reverberation time derived from the impulse responses measured on bricks. These values are obtained by calculating the energy decay curve respectively with the energy detection method and with the compensated Schroeder's backward integration method. For this comparison, as reverberation time $T_{20}$ is used instead of $T_{30}$, due to the reduced dynamic range of the structural impulse responses that in general occurs. Figures 4.3 and 4.4 show the same results for the measurements performed on the concrete slab.

A common observation for both the set of measurements could be made about the irregularity of the values of reverberation time extracted with the compensated Schroeder's integration method. The peak in the graphs of reverberation time $T_{20}$ in figures 4.1b and 4.3b corresponds to those cases when the estimation on the background noise reduces the evaluable dynamic range. In figure 4.5 is presented an example of filtered impulse response that returns a peak value in the graphs. With a wrong estimation of the background noise, the calculated integral underestimates the energy decay: in this case the reverberation time evaluated through the extrapolation by a linear fitting over the energy decay between -5 dB and -25 dB returns an overestimated value. In the example, to obtain a good value of reverberation time, the dynamic range for the estimation has to be reduced to 20

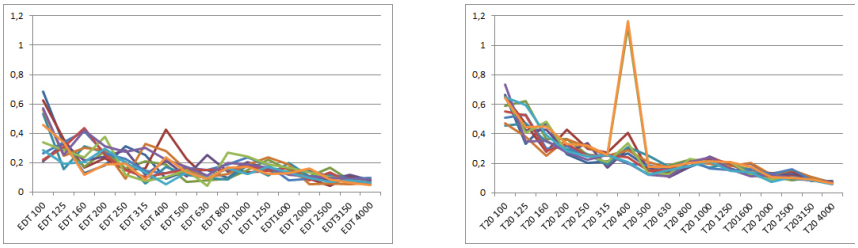


(a) EDT (b) $T_{20}$

Figure 4.1: Brick wall. Energy decay curve calculated with the compensated Schroeder's integration method.

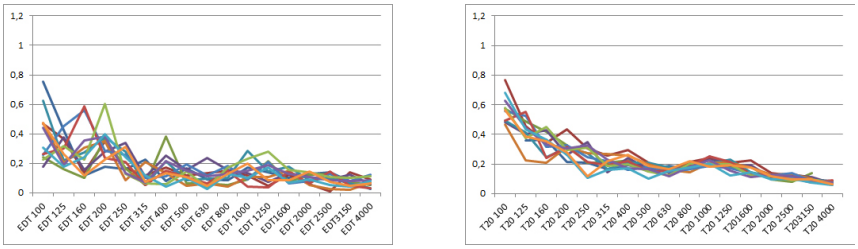


(a) EDT (b) $T_{20}$

Figure 4.2: Brick wall. Energy decay curve calculated with the preprocessed energy detection method.

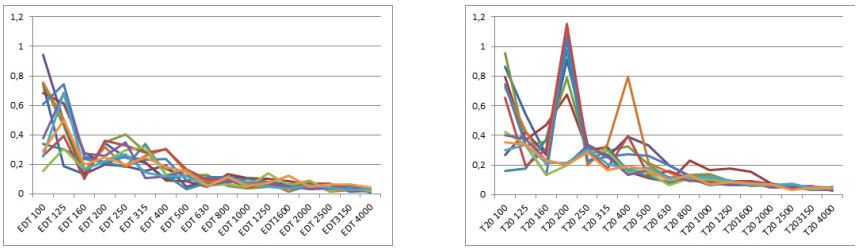


(a) EDT (b) $T_{20}$

Figure 4.3: Slab. Energy decay curve calculated with the compensated Schroeder's integration method.

dB, corresponding to a reverberation time $T_{15}$.

On the other hand the independence from the estimation of the background noise of the new proposed method for the energy decay curve extraction doesn't presents this problem and typically returns a value of reverberation time that is representative of the energy decay. Moreover this independence doesn't reduce the evaluable dynamic range (see figg. 4.2b 4.4b).

Figures 4.1a, 4.2a, 4.3a and 4.4a also show the resulting early decay time evaluated in each third octave band with both the energy decay curve extraction methods. In all cases, the evaluated early decay time could be considered representative of the early energy decay. The problem of a good evaluation of the first decay using the compensated Schroeder's integration method (presented in chapter 3), here doesn't exist. In fact, here there isn't a different behaviour of the first reflections compared to the rest of the energy decay, but the decay is typically linear.

The steep energy decay that is typical of the structural impulse responses is well detected by both methods (fig. 4.6). Only a further observation could be made: in some cases (in general yet so limited), the dependence of the compensated Schroeder's backward integration method on the estimation of the background noise and the consequent reduction of the evaluable dynamic range, could reduce the range so significantly that it could become so small that no criteria can be evaluated. One recent example could be found in [58] where the authors, using the Schroeder's backward integration method, choose to extract the reverberation time $T_5$. Using the new proposed method over the same impulse responses the useful dynamic range could be sensibly improved.

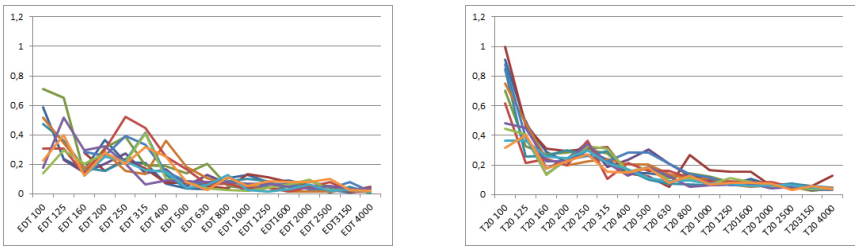


(a) EDT (b) $T_{20}$

Figure 4.4: Slab. Energy decay curve calculated with the preprocessed energy detection method.

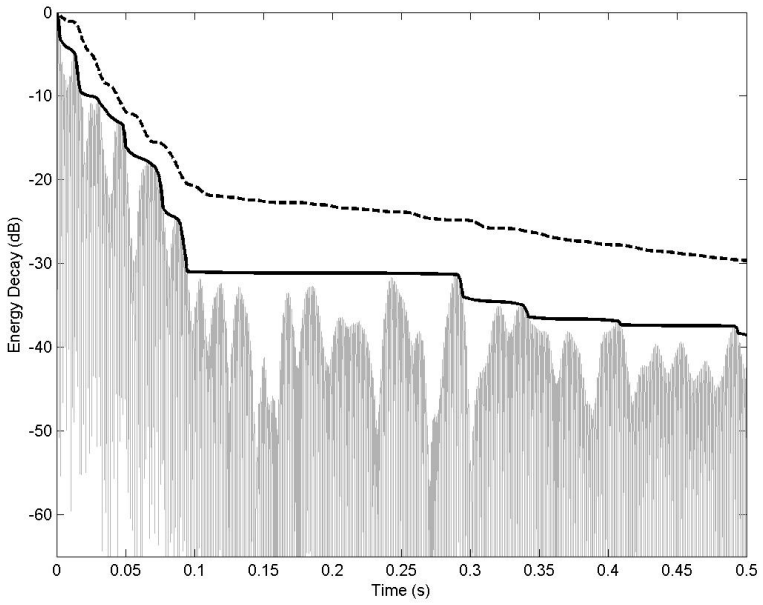


Figure 4.5: Example of structural impulse response (grey curve) analysed with both the energy decay curve extraction methods. Solid line: preprocessed energy detection method. Dashed line: compensated Schroeder's integration method. The compensated Schroeder's backward integration method underestimates the energy decay due to a poor estimation of the background noise.

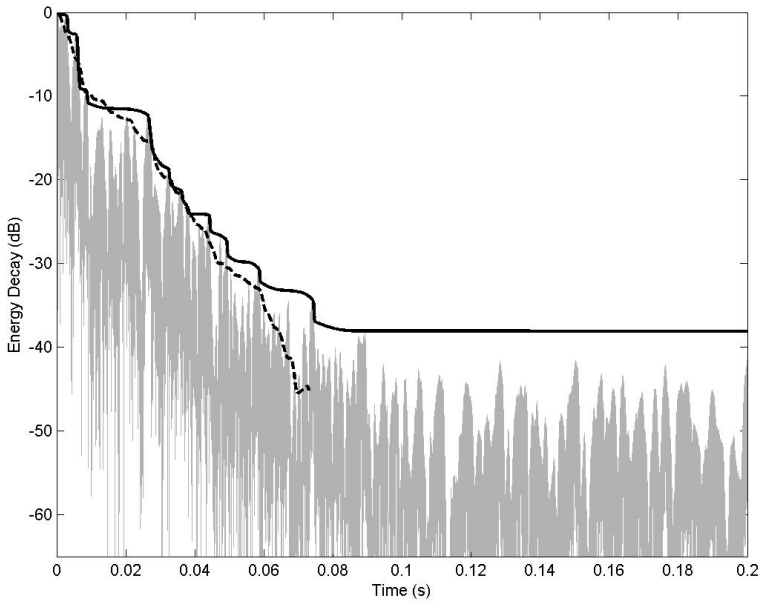


Figure 4.6: Example of structural impulse response (grey curve) with both the energy decay curve extraction methods. Solid line: preprocessed energy detection method. Dashed line: compensated Schroeder's integration method. Both the method return a good evaluation of the first part of the decay.

# Chapter 5

# On the statistical analysis of distributed measurements (in Italian historical theatres)

The aim of this chapter is to evaluate the statistical representativeness of the values of reverberation time and of the EDT extracted with the compensated Schroeder's backward integration method and with the new proposed method. In particular the idea is to define whether the mean value and the standard deviation of the measured values of reverberation time and EDT are representative for the overall characterization of the hall under study. In this case an interesting indication concerns the minimum ratio between the number of measurements and the total number of listening positions of a hall needed to extract these representative mean value and standard deviation.

As explained in the chapter 3, for nine Italian historical theatres the measurements were performed in each listening position in the audience, in the boxes and in the gallery. For this reason this statistical evaluation is specialized for the measurements in the Italian historical theatres.

The first step is to analyse whether the reverberation time and EDT values extracted present a gaussian distribution: this evaluation is made performing some different normality tests over all the measurements separately in the audience, in the boxes and in the gallery. The second step is to select the criteria that result normally distributed and then evaluate which receiver's selection (subset) preserve this property (each receiver selection is different in cardinality and spatial distribution). The third step is to make some evaluations for those criteria that do not result normally distributed.

## 5.1 Normality tests

Tests for normality were carried out for each parameter like in previous literature [59, 60], using statistical moments and the empirical cumulative distribution function $F(z_i)$:

$$F(z_i) = \frac{1}{\sqrt{2\pi}} \int_{-\infty}^{z_i} e^{-\frac{t^2}{2}}\, dt \tag{5.1}$$

where $z_i$ are the $i$-th measured data of the studied configuration, ordered and normalized ($i = 1, \ldots, N$).

**Anderson-Darling statistic (ADT)**

$$A^2 = \lambda \left[ -\sum_{i=1}^{N} (2n-1) \frac{ln(F(z_i)) + ln(1 - F(z_{N+1-i})}{N} - N \right] \tag{5.2}$$

where

$$\lambda = 1 + \frac{0.75}{N} + \frac{2.25}{N^2} \tag{5.3}$$

**Kolmogorov-Smirnov statistic (KS)**

$$D = \max\left(D^+, D^-\right) \tag{5.4}$$

where:

$$D^+ = \max_{1 \le i \le n} \left[ \left( \frac{i}{n} \right) - F(z_i) \right] \tag{5.5}$$

$$D^- = \max_{1 \le i \le n} \left[ F(z_i) - \frac{(i-1)}{n} \right] \tag{5.6}$$

**Pearson $\chi^2$ (CHI)**

$$\chi^2 = \sum_{i=1}^{n} \frac{(z_i - \mu)^2}{\mu} \tag{5.7}$$

**Jarqe-Bera statistics (JB)**

$$JB = \frac{N}{6} \left[ S^2 + \frac{1}{4}(K-3)^2 \right] \tag{5.8}$$

where $S$ is the skewness and $K$ is the kurtosis.

If the calculated statistic exceeds the critical value (a type I error of $\alpha = 0.05$ is assumed), the so called *null hypothesis* of normality may be rejected.

## 5.2 Estimation of normally distributed criteria through a selection of measurements

The normality tests performed over the reverberation time ($T_{30}$) show that values are normally distributed. Considering the $T_{30}$ value measured in one general listening position, we can call this value $x$ and consider it as one observation of the random variable $X$. From the normality test results we can say that:

$$X \sim N(\mu, \sigma^2) \tag{5.9}$$

where

$\mu$ is the mean value of the population;

$\sigma$ is the standard deviation of the population.

It is important to note that in this analysis both $\mu$ and $\sigma$ are known, but in general both of them are unknown; in this particular case we have a complete characterization of the area of the theatre under test, but our scope is to find a relation between the value extracted from all the measurements and the one extracted from a selection of receiver positions, so this work could be useful to reduce the number of measurements. The number $n$ of measurements required for a good characterization is unknown. Statistically speaking $n$ is the number of samples that we consider and $x_1, x_2, \ldots, x_n$ are the observations of the random variables $X_1, X_2, \ldots, X_n$ identically distributed with the same distribution of $X$. For the point estimation, the target is to find the real value of the unknown parameter through one single value. Formally speaking, the problem is to choose $t = g(x_1, x_2, \ldots, x_n)$ that gives the real value of the unknown parameter and that is called *estimation*. The random variable $T = g(X_1, X_2, \ldots, X_n)$ of which $t$ is the realization over the sample selected is called *estimator*. In this terms, $T$ is a random variable with its own sample distribution.

Different methods exist for the point estimation to find estimation/estimator for parameters in different situation.

Here we want to estimate the mean value and the variance of a normally distributed population.

It is known that if the sample $x_1, x_2, \ldots, x_n$ is extracted from a normal population, so $X_i \sim N(\mu, \sigma^2)$ for each $i = 1, \ldots, n$, then $\bar{X}$ and $S'^2$ are optimal estimators respectively for $\mu$ and $\sigma$ in the class of the correct estimator. $\bar{X}$ is the sample mean and is given by

$$\bar{X} = \frac{1}{n}\sum_{i=1}^{n} X_i \tag{5.10}$$

and $S'^2$ is the correct sample variance, given by

$$S'^2 = S^2 \frac{n}{n-1} \tag{5.11}$$

where

$$S^2 = \frac{1}{n}\sum_{i=1}^{n}(X_i - \bar{X})^2 \tag{5.12}$$

substituting equation 5.12 in 5.11, we can rewrite the correct sample variance as

$$S'^2 = \frac{1}{n-1}\sum_{i=1}^{n}(X_i - \bar{X})^2 \tag{5.13}$$

and rename the correct sample variance as $S^2$.

The main properties of the sample mean and variance are:

- $E(\bar{X}) = \mu$
- $V(\bar{X}) = \frac{\sigma^2}{n}$
- $E(S^2) = \sigma^2$

The distribution of the sample statistics of a normal distributed sample are known and are:

$$\bar{X} \sim N(\mu, \frac{\sigma^2}{n}) \tag{5.14}$$

$$\frac{(n-1)S^2}{\sigma^2} \sim \chi^2_{n-1} \tag{5.15}$$

where $\chi^2_{n-1}$ is the $\chi^2$ distribution with $n-1$ degree of freedom.

Now we have to estimate the mean and the variance for normal sample; in this case both the mean and the variance are unknown. To estimate the mean we can consider the statistics

$$T = \frac{\bar{X} - \mu}{S/\sqrt{n}} \sim t_{n-1} \tag{5.16}$$

where $t_{n-1}$ is the student-t distribution with $n-1$ degrees of freedom.
It is possible to find the confidence interval with confidence level $1-\alpha$:

$$\left[\bar{x} - \frac{s}{\sqrt{n}} t_{n-1,\alpha/2}; \bar{x} + \frac{s}{\sqrt{n}} t_{n-1,\alpha/2}\right] \tag{5.17}$$

The estimation of the variance starts from equation 5.15 and we can find that the confidence interval with confidence level $1-\alpha$ for $\sigma^2$ is:

$$\left[\frac{(n-1)s^2}{\chi^2_{n-1,\alpha/2}}; \frac{(n-1)s^2}{\chi^2_{n-1,1-\alpha/2}}\right] \tag{5.18}$$

in the case of the variance, also the unilateral confidence interval could be interesting, that are

$$\left[0; \frac{(n-1)s^2}{\chi^2_{n-1,1-\alpha}}\right] \tag{5.19}$$

$$\left[\frac{(n-1)s^2}{\chi^2_{n-1,\alpha}}; +\infty\right) \tag{5.20}$$

With these results is possible to identify the confidence interval for both mean and variance.

Acoustically speaking, now we can choose a subset of measurements of cardinality $n$, calculate the sample mean and variance and then calculate the corresponding confidential interval with a certain confidence level. Now we can compare the confidence limit of the mean and of the variance combined with the JND of the criterion under test.

## 5.3 Experimental results: normality test

In this section the evaluations explained in section 5.1 one are applied to the values of reverberation time $T_{20}$ and EDT calculated with the compensated Schroeder's integral and with the Energy Detection Method. This evaluation is particularly interesting when the aim of the work is the characterization of a theatre. In fact, theatres typically have lots of listening positions and, expecially considering the Italian historical theatres, the listening position are distributed in several areas of the theatre. For Italian historical theatres it is possible to divide the whole volume open to the the public of the theatre in three main regions: the audience, the boxes and the gallery.

The figures 5.2 and 5.4 present the results of the normality tests evaluated over the criteria extracted with the energy detection method (EDM) for each theatre

| TEST | EDT 63 | EDT 125 | EDT 250 | EDT 500 | EDT 1000 | EDT 2000 | EDT 4000 |
|---|---|---|---|---|---|---|---|
| ADT | 0 | 1 | 1 | 1 | 1 | 1 | 1 |
| KS | 0 | 0 | 0 | 0 | 1 | 0 | 1 |
| CHI | 0 | 1 | 1 | 0 | 1 | 0 | 0 |
| JB | 1 | 1 | 1 | 1 | 1 | 1 | 1 |

(a) Audience.

| TEST | EDT 63 | EDT 125 | EDT 250 | EDT 500 | EDT 1000 | EDT 2000 | EDT 4000 |
|---|---|---|---|---|---|---|---|
| ADT | 1 | 0 | 1 | 0 | 1 | 1 | 1 |
| KS | 0 | 0 | 0 | 0 | 0 | 0 | 1 |
| CHI | 1 | 0 | 1 | 0 | 1 | 1 | 0 |
| JB | 1 | 1 | 0 | 0 | 1 | 1 | 1 |

(b) Boxes and gallery.

| TEST | EDT 63 | EDT 125 | EDT 250 | EDT 500 | EDT 1000 | EDT 2000 | EDT 4000 |
|---|---|---|---|---|---|---|---|
| ADT | 0 | 0 | 1 | 0 | 1 | 1 | 1 |
| KS | 0 | 0 | 0 | 0 | 0 | 0 | 0 |
| CHI | 0 | 0 | 0 | 0 | 0 | 1 | 0 |
| JB | 1 | 0 | 0 | 0 | 0 | 1 | 1 |

(c) Only boxes.

Figure 5.1: Example of results of each normality test in the different areas.

considering separately the audience, the boxes and the boxes and gallery together. This choice is due to the particular configuration of the gallery in the Italian historical theatres: while the boxes present a closed volume, the gallery presents an open volume. The statistics were also performed for all the used sound source positions to evaluate the incidence of the position of the source on the stage in the normality evaluations.

Figures 5.3 and 5.5 show the same evaluations performed over the criteria extracted with the compensated Schroeder's integration method (compSCH).

The results in the figures 5.2 - 5.5 have been performed applying the four considered normality tests (see sec. 5.1) as reported for example in figure 5.1. Then for each theatre and each source position figures 5.2 - 5.5 have been realized considering the criterion in the selected octave band normally distributed if at least three out of four of the normality tests were passed. For example the tests shown in figure 5.1 correspond to the first line of figure 5.2a.

The normality tests reveal that in general the reverberation time $T_{20}$ calculated from the impulse responses measured in the audience could be considered normally distributed, expecially when calculated with the compensated Schroeder's integra-

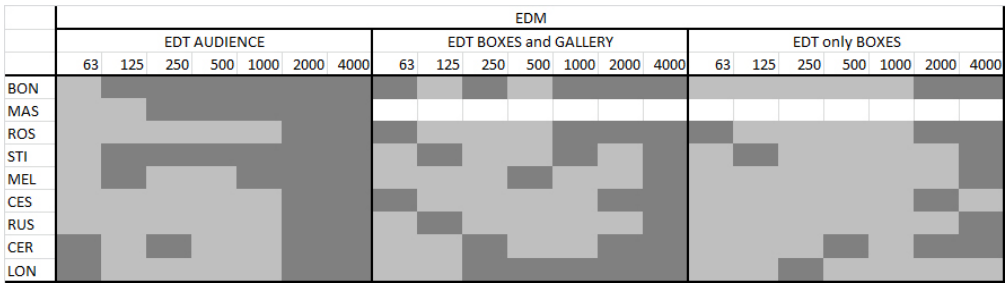


(a) Front source.

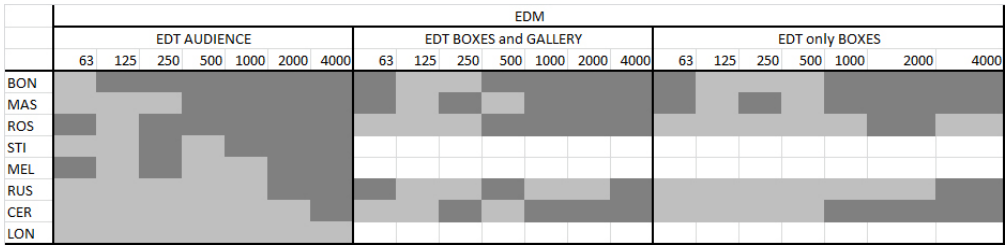


(b) Rear source.

Figure 5.2: Combined normality tests results for the EDT extracted with the preprocessed energy detection method.

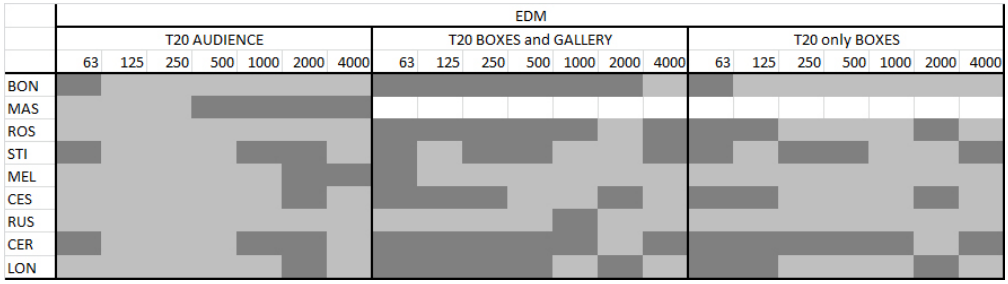


(a) Front source.

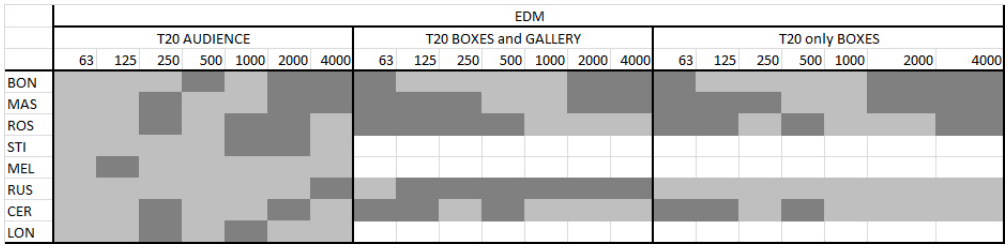


(b) Rear source.

Figure 5.3: Combined normality tests results for the $T_{20}$ extracted with the preprocessed energy detection method.

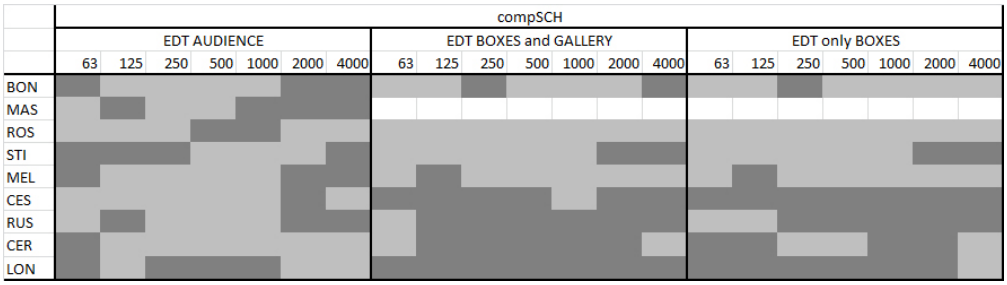


(a) Front source.

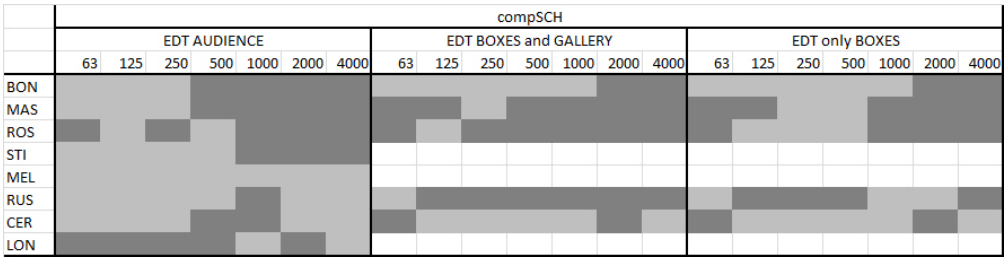


(b) Rear source.

Figure 5.4: Combined normality tests results for the EDT extracted with the compensated Schroeder's integration method method.

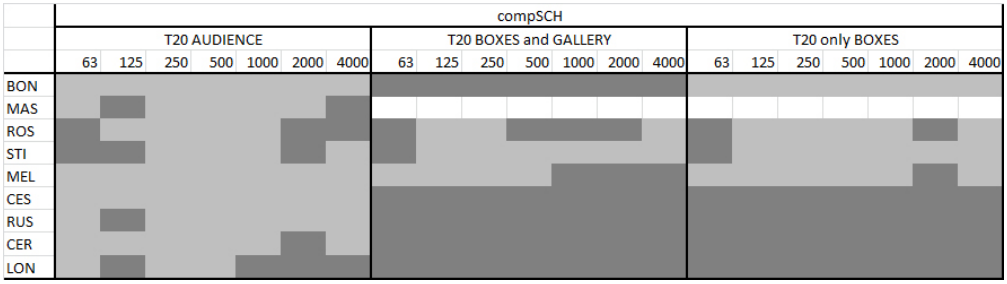


(a) Front source.

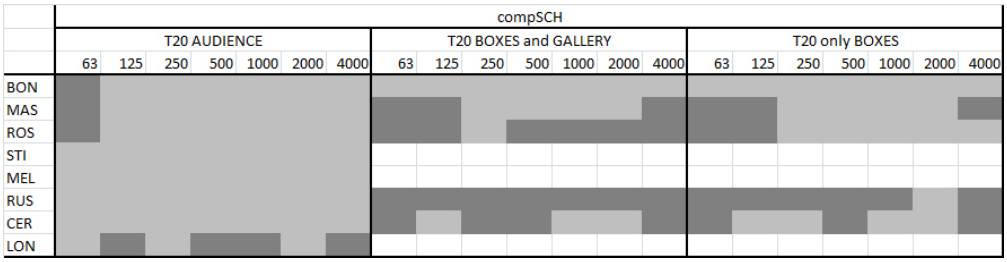


(b) Rear source.

Figure 5.5: Combined normality tests results for the $T_{20}$ extracted with the compensated Schroeder's integration method method.

tion method and when the source is positioned in the middle of the stage. The fact that with the rear source position the criterion results more regularly distributed could be explained considering that in this case the audience lies in a space region where the average acoustic field can be considered diffuse. The fact that the compSCH method returns a more regular distribution of the parameter related to the EDM is well correlated with the construction of the decay curve on the impulse response; as previously discussed, the EDM returns more detailed decay curve which implies a wider variation of the reverberation time extracted in a particular space.

Considering the reverberation time $T_{20}$ calculated in the boxes and in the gallery, in general it is not possible to identify a normal distribution that can characterize the whole set of values. When only the impulse responses measured in the boxes are considered the conclusion is the same.

Different evaluations can be drawn for the early decay time. In general, the EDT calculated from the impulse response measured in the audience seems not to be normally distributed. But in this case it is possible to make some interesting evaluations considering the different theatres. As shown before, the theatres are presented in decreasing order considering the total volume. It is possible to note that, when the sound source is positioned in the middle of the stage, the EDT calculated over the energy decay curve extracted with the EDM becomes normally distributed moving towards smaller sizes of the theatres. In other words, referring to figure 5.2a, the EDT calculated for the audience of the Bonci theatre, that is the greater one, is not normally distributed, while the same criterion calculated for the audience of Petrella Theatre, that is the smaller one, is normally distributed for all the considered octave bands.

Considering the characteristics of the new proposed method for the extraction of the energy decay curve and the relative features of the EDT calculated from that, the fact that the EDT results normally distributed or not, could be related to the distribution of the first reflections. If the first reflections are well separated, their distribution is deterministic and strictly depends on the measurement position; in the other case, the distribution of reflections is statistical as in a diffuse field. Thus in the first case the distribution of the criterion results not well described in a statistical sense, while in the second case it is.

This idea is well supported by the results measured for the Italian historical theatres presented here, and specifically the ones obtained with the rear source position (fig. 5.2a).

The normality test performed here also return that the EDT calculated for boxes and gallery together are not normally distributed. Eliminating the values calculated for the gallery, only the ones obtained with the EDM for the extraction of the decay curve and measured with the front source becomes normally dis-

tributed. This could be explained considering the relative position of the gallery related to the position of the stage. With the rear position, the source is not 'visible' from the gallery, while it is for the front position. In other words for the rear source it is possible to consider the gallery as an area with its own 'acoustic field' depending on the acoustic field of the whole theatre while for the front source the acoustics in the gallery is well dependent on the acoustic field of the rest of the theatre.

# Chapter 6

# Final considerations

Starting from the analysis of the previous literature concerning the methods for the extraction of energy decay curve, and in particular from the still existing problems, a new energy decay extraction method has been proposed. The new method has been implemented in a Matlab© toolbox. Then, its performance has been systematically tested versus the most accredited literature method, the Schroeder's backward integration method with noise subtraction, truncation and correction (see section 1.3).

The values of EDT and reverberation time extracted from the energy decay curves calculated with both the methods have been compared in terms of the values themselves and in terms of their statistical representativeness. In particular, for the nine Italian historical theatres treated in chapter 3, the criteria have been compared to the results provided by Barron in his analysis of 17 English concert halls [40].

The comparison between the two extraction methods underlines that both return a comparable value of the reverberation time $T_{30}$. Decreasing the range of evaluation, the two methods reveal increasing differences; in particular, the main differences are in the first part of the decay, where the EDT is evaluated.

These differences are due to the fact that the proposed extraction method returns a more detailed curve, where the different parts of the energy decay can be clearly distinguished. On one hand, this can be read as an ability of the new method to identify the decay of the first reflections and thus return a value of EDT based on these reflections only; in some cases it can be significantly different from the reverberation time $T_{30}$ calculated on the same impulse response. This is often the case in Italian historical theatres, where the first reflections are strong and distinct from the late reverberation tail. On the other hand, this feature of the new method may be useful to identify different decay slopes in case of multi-rate decays (for example in coupled spaces), being less computationally demanding than the Bayesian methods. Both these useful characteristics are consequences

of the fact that the new method returns a "locally" defined energy decay curve, whereas the Schroeder's method accumulates energy from the tail to the beginning of the impulse response.

Another characteristic of the new proposed method for the energy decay extraction curve is its independence on the background noise estimation. On the contrary, the Schroeder's backward integration method needs a careful estimation of the background noise and sometimes a poor estimation of it may affect the final result.

Due to the detailed evaluation of the first part of the decay, in particular in the case of impulse responses measured in the Italian historical theatres, the EDT values extracted with the new proposed method present a wide range of values. This permits to extend Barron's analysis also to this peculiar type of halls (Italian opera houses) in order to find a direct correspondence between the perceptive significance of the EDT and the architectural features of the theatres. Moreover, it is also possible to extend the Barron's evaluations concerning the trend of the EDT values related to the source-receiver distance by redefining the concept of distance as a term related to other acoustical parameters.

The independence from the background noise of the energy decay curve extracted with the new proposed method is useful in case of structural impulse responses. In fact they typically present a reduced dynamic range, so that a poor estimation of the background noise when using the compensated Schroeder's backward integration method may dramatically reduce the evaluable dynamic range.

The final part of the present work is devoted to the statistical analysis of a large set of measurements done in nine Italian historical theatres. Both the energy decay extraction methods permit to well describe the values of reverberation time in terms of statistical distribution.

For the compensated Schroeder's integration method, the statistical results for EDT values are similar to those obtained from the reverberation time, while the new proposed method seems to reflect the behaviour of the first reflections in the normality test results.

# Bibliography


[1] UNI EN ISO 3382: 2009, "Acoustics - Measurement of room acoustic parameters" (2009).

[2] B.F.G. Katz, International round robin on room acoustical impulse response analysis software, Acoustics Research Letters Online, 5, 158, 2004.

[3] W.C. Sabine, "Collected papers on acoustics", 1922.

[4] Meyer, E., "Beitage zur Untersuchung des Nachhalles", *Elektrische Nachrichtentechnik (ENT)*, 4(3), 135–139, 1927.

[5] F.V. Hunt, "Apparatus and technique for reverberation measurements", *J. Acoust. Soc. Am*, 8, 1936.

[6] V.O. Knudsen, "Resonance in small rooms", *J. Acoust. Soc. Am*, 4, 20–37, 1932.

[7] H.E. Hollmann, T.H. Schultes, "Raumakustische Kippschwingungen", *Elektrische Nachrichtentechnik (ENT)*, November 1931.

[8] J.T. Broch, "On the Use of Warble Tone and Random Noise for Acoustic Measurement Purposes", Brüel and Kjær Technical Review. No. 4, 1966.

[9] E. Meyer, L. Keidel, "Rohrenvoltmeter mit logarithmischer Anzeige und seine Anwendungen in der Akustik", *Elektrische Nachrichtentechnik (ENT)*, 12(2), 37–46, 1935.

[10] E.C. Wente, E.H. Bedell, "A Chronographic Method of Measuring Reverberation Time", *J. Acoust. Soc. Am.*, 422, 1930.

[11] H.F. Olson, B. Kreuzer, "The Reverberation Time Bridge: an instrumental method for measuring reverberation time", *J. Acoust. Soc. Am.*, 1, 78–82, 1930.

[12] S. Ballantine, "Logarithmic Recorder for Frequency Response Measurements at Audio Frequencies", *J. Acoust. Soc. Am.*, 1(5), 10, 1933.

[13] E.H. Bedell, K.D. Swartzel, "High speed level recorder for acoustic measurements", *J. Acoust. Soc. Am.*, 6(3), 130–132, 1935.

[14] P.M. Morse, R. Bolt, "Sound waves in rooms", Reviews of Modern Phisics, 78–80, 16(2), 1944.

[15] V.L. Chrisler, C.E. Miller, "Some of the factors which affect the measurement of sound absorption", BIPM, 175–185.

[16] S. Lifshitz, "Apparent duration of sound perception and musical optimum reverberation", *J. Acoust. Soc. Am*, 7, 213–221, 1936.

[17] W. Richings, "A new sound level meter using transistors", Proc. of the 3rd International Congress on Acoustics, **2**, 717, Stuttgart, 1959.

[18] S.B. Pedersen, "A logarithmic attenuator", Proc. of the 3rd International Congress on Acoustics, **2**, 720–723, Stuttgart, 1959.

[19] J.T. Broch, V.N. Jensen, "On the Measurement of Reverberation", Brüel and Kjær Technical Review. No. 4, 1966.

[20] M. Schroeder, "New method of measuring reverberation time", *J. Acoust. Soc. Am.*, 37, 407–412, 1965. See also *J. Acoust. Soc. Am.* 38, 359-361, 1965; and *J. Acoust. Soc. Am.* 40, 549-551, 1966.

[21] Y. Hirata, "A method of eliminating noise in power response", *J. Sound Vib.*, 82(4), 593-595, 1982.

[22] M. Vorländer, H. Bietz, "Comparison of methods for measuring reverberation time", *Acustica*, 80, 205–215, 1994.

[23] T. Cox, F. F. Li, P. Darlington, "Extracting room reverberation time from speech using artificial neural networks", *J. Audio Eng. Soc.*, 49, 219–230, 2001.

[24] J. Vieira, "Automatic estimation of Reverberation Time", Proceedings of the AES 116th International Convention, Berlin, Germany, 2004.

[25] D. Morgan, "A parametric error analysis of the backward integration method for reverberation time estimation", *J. Acoust. Soc. Am.*, 101, 2686–2693, 1997.

[26] M. Guski, M. Vorländer,"Comparison of Noise Compensation Methods for Room Acoustic Impulse Response Evaluations", *Acta Acous.*, 100, 320-327, 2014.

[27] L. Faiget, R. Ruiz, C. Legros, "The true duration of the impulse response used to estimate reverberation time", *Acoustics, Speech, and Signal Processing, 1996. ICASSP-96. Conference Proceedings., 1996 IEEE International Conference on*, Vol. 2, 913-916, 1996.

[28] A. Lundeby, T. E. Vigran, H. Bietz, and M. Vorländer, "Uncertainties of Measurements in Room Acoustics", *Appl. Acoust.*, 81, 344–355, 1995.

[29] W. T. Chu, "Comparison of reverberation measurements using Schroeder's impulse method and decay-curve averaging method", *J. Acoust. Soc. Am.*, 63(5), 1444–1450, 1978.

[30] F. Satoh, Y. Hidaka, and H. Tachibana, "Reverberation time directly obtained from squared impulse response envelope", *Proc. Int. Congr. Acoust.*, Seattle, WA, 2755–2756, 1998.

[31] N. Xiang, "Evaluation of reverberation times using a nonlinear regression approach", *J. Acoust. Soc. Am.*, 98, 2112–2121, 1995.

[32] N. Xiang, P.M. Goggans, "Evaluation of decay times in coupled spaces: Bayesian parameter estimation", *J. Acoust. Soc. Am.*, 110(3), 1415-1424 , 2001.

[33] N. Xiang, P. M. Goggans, "Evaluation of decay times in coupled spaces: Bayesian decay model selection", *J. Acoust. Soc. Am.*, 113, 2685–2697, 2003.

[34] N. Xiang, P.M. Goggans, T. Jasa, M. Kleiner, "Evaluation of decay times in coupled spaces: Reliability analysis of Bayesian decay time estimation", *J. Acoust. Soc. Am.*, 117(6), 3707-3715, 2005.

[35] N. Xiang, T. Jasa, "Evaluation of decay times in coupled spaces: An efficient search algorithm within the Bayesian framework", *J. Acoust. Soc. Am.*, 120(6), 3744-3749, 2006.

[36] M. Karjalainen, P. Antsalo, A. Makivirta, T. Peltonen, and V. Valimaki, "Estimation of modal decay parameters from noisy response measurements", *J. Audio Eng. Soc.*, 50, 867–879, 2002.

[37] B.S. Atal, M.R. Schroeder, G.M. Sessler, "Subjective Reverberation Time and Its Relation to Sound Decay", *Bell telephone system technical publications*, 5078, 1966.

[38] M.R. Schroeder, B.S. Atal, G.M. Sessler, J.E. West, "Acoustical Measurements in Philharmonic Hall (New York)", *J. Acoust. Soc. Am.*, 40(2), 434-440, 1966.

[39] V.L. Jordan, "Acoustical Criteria for Auditoriums and Their Relation to Model Techniques", *J. Acoust. Soc. Am.*, 47(2), 408-412, 1969.

[40] M. Barron, L.J. Lee, "Interpretation of early decay time in concert auditoria.", *Acustica*, 81, 320-331, 1995.

[41] M. Barron, "Objective assessment of concert hall acoustic using Temporal Energy Analysis", *Appl. Acoust.*, 74, 936-944, 2013.

[42] J.S. Bradley, "Review of objective room acoustics measures and future needs", *Appl. Acoust.*, 72, 713-720, 2011.

[43] J.S. Bradley, "An international comparison of room acoustic measurements systems", In *IRC Internal Report no. 714*, January 1996.

[44] H. Urkowitz, "Energy detection of unknown deterministic signal", *Proceedings of the IEEE*, 55, 523–531, 1967.

[45] F.N. Frisch, R.E. Carlson, "Monotone piecewise cubic interpolation", *SIAM J. Numer. Anal.*, 17(2), 238-246, 1980.

[46] F. Jacobsen, "A note on acoustic decay measurements", *J. Sound Vib.*, 115(1), 163-170, 1987.

[47] F. Jacobsen, J.H. Rindel, "Time reversed decay measurements", *J. Sound Vib.*, 117(1), 187-190, 1987.

[48] M. Kob, M. Vorländer, "Band filters and short reverberation time", *Acustica-Acta Acustica*, 86, 350-357, 2000.

[49] M.A. Sobreira-Seoane, D.P. Cabo, F. Jacobsen, "The influence of the group delay of digital filters on acoustic decay measurements", *Acta Acustica*, 73, 877-883, 2012.

[50] D.P. Cabo, M.A. Sobreira-Seoane, F. Jacobsen, "A Monte-Carlo investigation of the uncertainty of acoustic decay measurements", *Proc. Euronoise 2012*, Prague, 2012.

[51] K. Hoshi, A. Marui, H. Okubo, H. Miyazaki, J. Kanda, M. Yairi, T. Asakura, Y. Yasuda, "A study on establishing benchmarks for acoustical parameters derived from impulse responses", *Proc. International Symposium on Room Acoustics (ISRA) 2013*, June 2013.

[52] M. Guski, M. Vorländer, "Noise compensation methods for room acoustical parameter evaluation", *Proc. International Symposium on Room Acoustics (ISRA) 2013*, June 2013.

[53] P. Dietrich, M. Guski, J. Klein, M. Muller-Trapet, M. Pollow, R. Scharrer M. Vorländer, "Measurements and Room Acoustic Analysis with the ITA-Toolbox for MATLAB", *Proc. of: 40th Italian (AIA) Annual Conference on Acoustics and the 39th German Annual Conference on Acoustics (DAGA)*, March 2013.

[54] F. Farneti, S. Van Riel, "L'architettura teatrale in Romagna 1757 - 1857", Firenze, Uniedit, 1975.

[55] UNI EN ISO 10140, "Acoustics - Laboratory measurement of sound insulation of building elements".

[56] UNI EN ISO 10848, "Acoustics - Laboratory measurement of the flanking transmission of airborne and impact sound between adjoining rooms".

[57] UNI EN 12354, "Building acoustics - Estimation of acoustic performance of buildings from the performance of elements".

[58] C. Hopkins, M. Robinson, "On the Evaluation of Decay Curves to Determine Structural Reverberation Times for Building Elements", *Acta Acous.*, 99, 226-244, 2013.

[59] X. Pelorson, J.P. Vian, J.D. Polack, "On the variability of room acoustical parameters: Reproducibility and statistical validity", *Appl. Acoust.*, 37(3), 175-198, 1992.

[60] T. Akama, H. Suzuki, A. Omoto, "Distribution of selected monaural acoustical parameters in concert halls", *Appl. Acoust.*, 71(6), 564-577, 2010.

# Acknowledgements

The measurements inside Italian historical theatres were performed within the project “Historic Theatres in Emilia Romagna”, conceived and funded by the Interdepartmental Center for Industrial Research - Building and Construction Unit of Alma Mater Studiorum - University of Bologna.